

HEAT CONDUCTION FROM TWO SPHERES

BY

Basim Jamil Mohammad Al-Minshawy

A Thesis Presented to the
DEANSHIP OF GRADUATE STUDIES

KING FAHD UNIVERSITY OF PETROLEUM & MINERALS

DHAHRAN, SAUDI ARABIA

In Partial Fulfillment of the
Requirements for the Degree of

MASTER OF SCIENCE

In

MATHEMATICS

May, 2010

KING FAHD UNIVERSITY OF PETROLEUM & MINERALS
DHAHRAN 31261, SAUDI ARABIA

DEANSHIP OF GRADUATE STUDIES

This thesis, written by Basim Jamil Mohammad Al-Minshawy under the direction of his thesis advisor and approved by his thesis committee, has been presented to and accepted by the Dean of Graduate Studies, in partial fulfillment of the requirements for the degree of MASTER OF SCIENCE IN MATHEMATICS.

Thesis Committee


Dr. Rajai S. Alassar (Advisor)



Dr. Mohamed A. El-Gebeily (Co-Advisor)



Dr. Hassan M. Badr (Member)


Dr. Ashfaq H. Bokhari (Member)


Dr. M. Tahir Mustafa (Member)



 Dr. Suliman S. Al-Homidan
(Department Chairman)


Dr. Salam A. Zummo
(Dean of Graduate Studies)

12/6/18

Date

To the children of Palestine

ACKNOWLEDGMENT

First and foremost, thanks to Allah who made me a Muslim, and gave me patience to accomplish this research.

Acknowledgment is due to King Fahd University of Petroleum & Minerals for supporting this research.

I would like to express my sincere gratitude and appreciation to my advisor, Dr. Rajai Alassar, for his constructive guidance, leadership, friendship, and his continuous support that can never be forgotten. I wish to extend my thanks and appreciation to my thesis co-advisor Dr. Mohamed El-Gebeily for his cooperation and constant help.

I also wish to extend my thanks and appreciation to my thesis committee Dr. Hassan Badr, Dr. Ashfaq Bokhari, and Dr. M. Tahir Mustafa for their suggestions and valuable comments. I am also grateful to all faculty members of the Department of Mathematics and Statistics for their help in enriching my academic experience.

I am grateful to my father, may Allah have mercy upon him who gave me strength in my life, my dear mother for her patience on parting and her invocation for me, and my beloved wife and children for their patience and sacrifices.

TABLE OF CONTENTES

	Page
ACKNOWLEDGEMENT.....	iv
LIST OF FIGURES	vi
ABSTRACT (ENGLISH)	viii
ABSTRACT (ARABIC)	ix
CHAPTER 1 INTRODUCTION AND LITERATURE REVIEW	1
CHAPTER 2 PRELIMINARIES	5
2.1 INTRODUCTION	5
2.2 THE HEAT FLUX	5
2.3 THE DIFFERENTIAL EQUATION OF HEAT CONDUCTION	6
CHAPTER 3 COORDINATE SYSTEMS	10
3.1 INTRODUCTION	10
3.2 ORTHOGONAL CURVILINER COORDINATES	10
3.3 BISPHERICAL COORDINATE SYSTEM	17
CHAPTER 4 PROBLEM OF HEAT CONDUCTION FROM TWO ADJACENT SPHERES	21
4.1 PROBLEM STATEMENT	21
4.2 ANALYTICAL STEADY-STATE SOLUTION	22
4.3 RATE OF HEAT TRANSFER	28
4.4 VERIFICATION OF THE SOLUTION	33
4.5 TRUNCATION ERROR	36
CHAPTER 5 EFFECT OF DIFFERENT PARAMETERS ON THE HEAT CONDUCTION PROCESS	38
5.1 INTRODUCTION	38
5.2 EFFECT OF THE TEMERATURE RATIO	38
5.3 EFFECT OF CENTER-TO-CENTER DISTANCE	45
5.4 EFFECT OF RADII RATIO	51
CHAPTER 6 CONCLUSION AND RECOMMENDATIONS	54
REFERENCES	55
VITA	59

LIST OF FIGURES

Figure 2.1 Nomenclature for the derivation of heat conduction equation	7
Figure 3.1 A curvilinear Coordinates System (u_1, u_2, u_3)	11
Figure 3.2 Differential Rectangular Parallelepiped	15
Figure 3.3 Surfaces of constant ξ	17
Figure 3.4 Surfaces of Constant θ	18
Figure 3.5 Bispherical coordinate system.....	19
Figure 3.6 Distance between the centers of the spheres	20
Figure 4.1 Problem configuration	21
Figure 4.2 Rectangular region for the problem	22
Figure 4.3 Rectangular region with dimensionless boundary conditions	23
Figure 4.4 Isotherms of the case $r_1 = 1, r_2 = 3, H = 5$, and $U_2 = 2$	27
Figure 4.5 Approximating a patch by a parallelogram	29
Figure 4.6 Isotherms for the case $r_1 = r_2 = 1, H = 4, U_2 = 1$	34
Figure 4.7 Variation of N_u along the surface (ξ_2) for the case $r_1 = r_2 = 1$ and $U_2 = 1$	35
Figure 4.8 Variation of $\overline{N_u}$ along the surface (ξ_2) for the case $r_1 = r_2 = 1$ and $U_2 = 1$	36
Figure 5.1 Variation of N_u along the surface (ξ_2) for the case $r_1 = 1, \ell = 3$, and $U_1 = 1$, (a) $r_2 = \frac{1}{4}$, (b) $r_2 = 1$, (c) $r_2 = 4$	40
Figure 5.2 Variation of $\overline{N_u}$ for the case $r_1 = 1, \ell = 3$, and (a) $r_2 = \frac{1}{4}$, (b) $r_2 = 1$, (c) $r_2 = 4$	41
Figure 5.3 Isotherms for the case $r_1 = 1, r_2 = 4$, and $H = 8$. (a) $U_2 = -3.0$, (b) $U_2 = -1.0$, (c) $U_2 = 0.0$, (d) $U_2 = 0.5$, (e) $U_2 = 3.0$	42
Figure 5.4 Isotherms for the case $r_1 = 1, r_2 = 1, H = 5$. (a) $U_2 = -3.0$, (b) $U_2 = -1.0$, (c) $U_2 = 0.0$, (d) $U_2 = 1.0$, (e) $U_2 = 3.0$	43

Figure 5.5 Isotherms for the case $r_1 = 1, r_2 = \frac{1}{4}, H = 4.25$.

(a) $U_2 = -3.0$, (b) $U_2 = -2.0$, (c) $U_2 = 0.0$, (d) $U_2 = 2$, (e) $U_2 = 3.0$ 44

Figure 5.6 Variation of N_u along the surface (ξ_2) for the case $r_1 = 1, U_2 = 1$

(a) $r_2 = \frac{1}{3}$, (b) $r_2 = 1$, (c) $r_2 = 3$ 46

Figure 5.7 Variation of $\overline{N_u}$ for the case $r_1 = 1, U_2 = 1$

(a) $r_2 = \frac{1}{3}$, (b) $r_2 = 1$, (c) $r_2 = 3$ 47

Figure 5.8 Isotherms for the case $r_1 = 1, r_2 = 3, U_2 = 1$.

(a) $H = 4.5$, (b) $H = 7$, (c) $H = 10$, (d) $H = 12$ 48

Figure 5.9 Isotherms for the case $r_1 = 1, r_2 = 1, U_2 = 1$.

(a) $H = 2.5$, (b) $H = 4$, (c) $H = 15$, (d) $H = 20$ 49

Figure 5.10 Isotherms for the case $r_1 = 1, r_2 = \frac{1}{3}, U_2 = 1$.

(a) $H = 2$, (b) $H = 5$, (c) $H = 10$, (d) $H = 20$ 50

Figure 5.11 Variation of N_u along the surface ξ_2 for the case $r_1 = 1, \ell = 2, U_2 = 1$... 51

Figure 5.12 Variation of $\overline{N_u}$ with r_2 for the case $r_1 = 1$, and $U_2 = 1$ 52

Figure 5.13. Isotherms for the case $r_1 = 1, \ell = 2, U_2 = 1$.

(a) $r_2 = 0.1$, (b) $r_2 = 0.5$, (c) $r_2 = 2$, (d) $r_2 = 4$ 53

THESIS ABSTRACT

Name: Basim Jamil Alminshawy
Title: Heat Conduction From Two Spheres
Major Field: Mathematics
Date of Degree: May, 2010

An exact solution of heat conduction from two spheres is obtained. The unconventional bispherical coordinates system is used to solve the problem. The two spheres may be of different diameters and located at any distance from each other. The effects of the axis ratio of the two spheres, the temperature ratio, and the center-to-center distance on the heat transfer coefficient (the famous Nusselt number) are studied.

ملخص الرسالة

الاسم: باسم جميل محمد المنشاوي

عنوان الرسالة: انتقال الحرارة بالتوصيل من كرتين

التخصص: رياضيات

تاريخ التخرج: جمادى الآخرة 1431 هجرية

في هذه الرسالة نجد حلاً تاماً لانتقال الحرارة بالتوصيل من كرتين متجاورتين في وسط ما. نستخدم في هذه الرسالة المحاور المزدوجة الكروية لحل المشكلة. الكرتان قد تكونان ذواتي أقطار مختلفة وعلى مسافات مختلفة من بعضهما البعض. نقوم بدراسة تأثير نسبة قطري الكرتين وتأثير نسبة حرارة الكرتين وتأثير المسافة بين مركزيهما على معامل انتقال الحرارة (رقم نزلت الشهير).

CHAPTER 1

INTRODUCTION AND LITERATURE REVIEW

The problem of heat transfer from a sphere has been investigated through numerous experimental and theoretical studies. On the early work on natural convection, the reader is referred to the work of Potter and Riley [1] who studied the convective heat transfer when a heated sphere is placed in a stagnant fluid. In particular, they numerically considered the situation of large values of a suitably defined Grashof number. Brown and Simpson [2] obtained a local unsteady solution at the upper pole of a sphere in which the temperature of the sphere is instantaneously raised above that of the surrounding ambient fluid. Their numerical solution reveals the development of a singularity at a finite time. The structure of this singularity is examined and its occurrence is interpreted as the time at which an eruption of the fluid from the sphere, ultimately resulting in the plume that is formed above it, first takes place. Geoola and Cornish [3] and [4] presented a numerical solution of steady-state and time-dependent free convection heat transfer from a solid sphere to an incompressible Newtonian fluid. They simultaneously solved the stream function, energy, and vorticity transport equations. Singh and Hasan [5] calculated numerically the flow properties of the free convection problem about an isothermally heated sphere by the series truncation method when Grashof number is of order unity. Riley [6] considered the free convection flow over the surface of a sphere whose temperature is suddenly raised to a higher constant value than its surroundings. He obtained a numerical solution of the Navier-Stokes equations for finite values of the Prandtl and Grashof numbers. Dudek et al. [7] presented an experimental measurement and a numerical calculation of both the steady-state and transient natural convection drag force around spheres at low Grashof number. The classic references related to forced and mixed convection past a sphere are those by Dennis and Walker [8] who studied the forced convection from a sphere placed in a steady uniform stream and investigated the phenomenon for Reynolds number up to 200 and Prandtl number up to 32768. Whitaker [9] collected forced convection heat transfer

data and used it to develop some minor variations on the traditional correlation. He determined heat transfer correlations for particularly flow past spheres. Dennis et al. [10] calculated the heat transfer due to forced convection from an isothermal sphere in a steady stream of viscous incompressible fluid for low values of Reynolds number and used series truncation method to solve the energy equation. Sayegh and Gauvin [11] solved numerically the coupled momentum and energy equations for variable property flow past a sphere and investigated the effect of large temperature differences on the heat transfer rate. Hieber and Gebhart [12] studied the mixed convection from a sphere and linearized the governing equation according to the matched asymptotic expansions of the perturbation theory and obtained a solution valid at small Grashof and Reynolds numbers. Acrivos [13] studied the mixed convection from a sphere and simplified the energy and momentum equations using the boundary layer approximation. Wong et al. [14] solved numerically the full steady Navier-Stokes and energy equations by the finite element method. Nguyen et al. [15] investigated numerically heat transfer associated with a spherical particle under simultaneous free and forced convection and solved the transient problem with internal thermal resistance.

Studies related to heat or mass transfer from a sphere in an oscillating free stream are represented by Drummond and Lyman [16] who used numerical methods for the solution of the Navier-Stokes and mass transport equations for a sphere in a sinusoidally oscillating flow with zero mean velocity. It was concluded that the mass transfer rate decreases with the decrease of the Strouhal number until reaching the value of 2 below which the rate is virtually independent of the Strouhal number. Ha and Yavuzkurt [17] studied heat transfer from a sphere in an oscillating free stream and showed that high-intensity forced acoustic oscillations can enhance gas-phase mass and heat transfer. Alassar and Bader [18] studied the heat convection from a heated sphere in an oscillating free stream for the two cases of forced and mixed convection regimes. Leung and Baroth [19] studied mass transfer from a sphere and reported that the presence of an acoustic field enhances heat transfer when the vibrational Reynolds number exceeds 400.

Several important applications require the solution of the equation of heat conduction from two spheres. Some examples are the heat transfer in stationary packed beds, dispersed particles under the influence of a spatially uniform electric field

(electrophoresis), and the thermo capillary motion of two spheres created by surface tension which develops when a temperature gradient is present around the bubbles. When the motion of the flowing fluid becomes slow, the solution of heat conduction represents a limiting case for forced convective heat/mass transfer around two spheres. In general, the results of the present work can be of use in applications where Biot and Rayleigh numbers are small and fluid heat conduction dominates the thermal resistance. Such conditions can be found at small length scales. Furthermore, the impact of pure conduction is sometimes required for the effect of, for example, buoyancy and other forces to be isolated and studied. All the results in [17] are resented in terms of $N_u - 2$. The value of two is the Nusselt number corresponding to pure heat conduction.

Heat conduction from a single sphere is a textbook problem. This simple problem was generalized by Alassar [20] who investigated the conduction heat transfer from spheroids by solving the steady version of the energy equation subject to the appropriate boundary conditions and showed that the solution for the sphere case can be obtained from his generalized results. Solomentsev et al. [21] found the asymptotic solution for Laplace equation over two equal nonconducting spheres of equal size when some field is applied perpendicular to the line of centers. Stoy [22] developed a solution procedure for the Laplace equation in bispherical coordinates for the flow past two spheres in a uniform external field. Dealing with Neumann boundary conditions, the determination of the coefficients of the orthogonal expansion is the central part of the work. It is interesting to know that the theoretically more complicated problem of convective heat transfer has been investigated, see for example Juncu [23]. In his work, Juncu studied numerically the problem of forced convection heat/mass transfer from two spheres which have the same initial temperature. Thau et al. [24] numerically solved the Navier-Stokes and energy equations for a pair of spheres in tandem arrangement at $Re=40$ for two different spacings using bispherical coordinates. Koromyslov and Grigor'ev [25] investigated an electrostatic interaction between two separate grounded uncharged perfectly conducting spheres of different radii in a uniform electrostatic field. Umemura et al. [26] and [27] investigated the effects of interaction of two burning identical spherical droplets with the same radius [26] and different sizes [27] of the same kind of fuel. They obtained the burning rate and the form of flame surface in the two-droplet case. Brzustowski et al. [28] found the burning rate of two interaction burning spherical

droplets of arbitrary size when the mass fraction of the diffusing fuel vapor at the droplets surfaces is the same.

In this study, a simple exact solution of heat conduction from two isothermal spheres is obtained. The unconventional bispherical coordinates system is used to solve the problem. The two spheres may be of different diameters and different temperatures, and may be located at any distance from each other. The necessity and importance of considering two spheres may be summarized by the following statements by Cornish [29].

1) It is well known that the minimum possible rate of heat (or mass) transfer from a single sphere contained within an infinite stagnant medium corresponds to a Nusselt (or Sherwood) number of two.

2) Frequently, however, in multi-particle situations such as fluidized beds, values of the Nusselt number less than two have been measured. A variety of reasons - such as backmixing – have been put forward to explain this apparent inconsistency. It does not seem to have been generally realized that for multi-particle situations the minimum theoretical value of the Nusselt number can be much less than two.

CHAPTER 2

PRELIMINARIES

2.1 INTRODUCTION

Heat transfer is the energy transport between materials due to a temperature difference. There are three modes of heat transfer namely, conduction, convection, and radiation. Conduction is the mode of heat transfer in which energy exchange takes place in solids or in fluids at rest (i.e., no convective motion resulting from the displacement of the macroscopic portion of the medium) from the region of high temperature to the region of low temperature. Molecules present in liquids and gases have freedom of motion, and by moving from a hot to a cold region, they carry energy with them. The transfer of heat from one region to another, due to such macroscopic motion in a liquid or gas, added to the energy transfer by conduction within the fluid, is called heat transfer by convection. All bodies emit thermal radiation at all temperatures. This is the only mode that does not require a material medium for heat transfer to occur. Temperature is a scalar quantity that describes the specific internal energy of the substance. The temperature distribution within a body is determined as a function of position and time, and then the heat flow in the body is computed from the laws relating heat flow to temperature gradient [36].

2.2 THE HEAT FLUX

It is important to quantify the amount of energy being transferred per unit time and for that we require the use of rate equations.

For heat conduction, the rate equation is known as *Fourier's law* [31], which is expressed for a homogeneous, isotropic solid (i.e., material on which thermal conductivity is independent of direction) as

$$\vec{q}(\vec{r}, t) = -k \vec{\nabla} T(\vec{r}, t) \quad (2.1)$$

where $\vec{\nabla} T(\vec{r}, t)$ is the temperature gradient vector normal to the surface ($^{\circ}\text{C} / \text{m}$), the heat flux vector $\vec{q}(\vec{r}, t)$ represents heat flow per unit time per unit area of the isothermal surface in the direction of decreasing temperature (W / m^2), and k is the thermal conductivity of the material which is a positive scalar quantity ($\text{W} / \text{m} \cdot ^{\circ}\text{C}$). The thermal conductivity k of the material is an important property which controls the rate of heat flow in the medium. There is a wide variation in the thermal conductivities of various materials. The highest value is given by pure metals and the lowest value by gases and vapors; the insulating materials and inorganic liquids have thermal conductivities that lie in between. Thermal conductivity also varies with temperature. For most pure metals, it decreases with increasing temperature whereas for gases it increases with increasing temperature. For most insulating materials, it increases with the increase of temperature.

In rectangular coordinate system (x, y, z), equation (2.1) is written as

$$\vec{q}(x, y, z, t) = -k \frac{\partial T}{\partial x} \hat{\mathbf{i}} - k \frac{\partial T}{\partial y} \hat{\mathbf{j}} - k \frac{\partial T}{\partial z} \hat{\mathbf{k}} \quad (2.2)$$

where $\hat{\mathbf{i}}$, $\hat{\mathbf{j}}$, and $\hat{\mathbf{k}}$ are the unit direction vectors along the x , y , and z directions, respectively.

2.3 THE DIFFERENTIAL EQUATION OF HEAT CONDUCTION

We now derive the differential equation of heat conduction for a stationary, homogeneous, isotropic solid with heat generation within the body. Heat generation may be due to nuclear, electrical, chemical, γ -ray, or other sources that may be a

function of time and/or position. The heat generation rate in the medium is denoted by the symbol $g(\vec{r}, t)$, and is given in the units W / m^3 [31].

We consider the energy balance equation for a small control volume V , illustrated in Figure 2.1, stated as

$$\left[\begin{array}{c} \text{Rate of heat entering through} \\ \text{the bounding surfaces of } V \end{array} \right] + \left[\begin{array}{c} \text{rate of energy} \\ \text{generation in } V \end{array} \right] = \left[\begin{array}{c} \text{rate of storage} \\ \text{of energy in } V \end{array} \right] \quad (2.3)$$

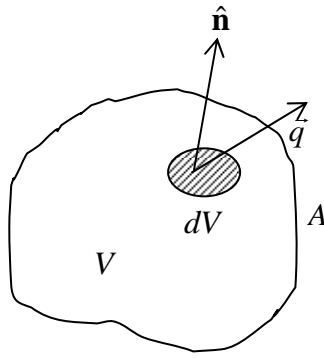


Figure 2.1. Nomenclature for the derivation of heat conduction equation

The various terms in this equation are evaluated as follows

$$\left[\begin{array}{c} \text{Rate of heat entering through} \\ \text{the bounding surfaces of } V \end{array} \right] = - \int_A \vec{q} \cdot \hat{n} dA = - \int_V \vec{\nabla} \cdot \vec{q} dV \quad (2.4)$$

where A is the surface area of the volume element V , \hat{n} is the outward drawn normal unit vector to the surface element dA , \vec{q} is the heat flux vector at dA ; here, the minus sign is included to ensure that the heat flow is into the volume element V .

$$\text{Rate of energy generation in } V = \int_V g(\vec{r}, t) dV \quad (2.5)$$

$$\text{Rate of energy storage in } V = \int_V \rho C_p \frac{\partial T(\vec{r}, t)}{\partial t} dV \quad (2.6)$$

where $\vec{\nabla}T(\vec{r},t)$ the temperature gradient vector normal to the isothermal surface, ρ is the density, and C_p is the specific heat.

The substitution of equations (2.4), (2.5), and (2.6) into equation (2.3) yields

$$\int_V \left[-\vec{\nabla} \cdot \vec{q}(\vec{r},t) + g(\vec{r},t) - \rho C_p \frac{\partial T(\vec{r},t)}{\partial t} \right] dV = 0 \quad (2.7)$$

Equation (2.7) is derived for an arbitrary small volume element V within the solid; hence the volume V may be chosen so small as to remove the integral. We obtain

$$-\vec{\nabla} \cdot \vec{q}(\vec{r},t) + g(\vec{r},t) = \rho C_p \frac{\partial T(\vec{r},t)}{\partial t} \quad (2.8)$$

Substituting equation (2.1) into equation (2.8) yields

$$\vec{\nabla} \cdot [k \vec{\nabla}T(\vec{r},t)] + g(\vec{r},t) = \rho C_p \frac{\partial T(\vec{r},t)}{\partial t} \quad (2.9)$$

When the thermal conductivity is assumed to be constant (i.e., independent of position and temperature), equation (2.9) simplifies to

$$\nabla^2 T(\vec{r},t) + \frac{1}{k} g(\vec{r},t) = \frac{1}{\alpha} \frac{\partial T(\vec{r},t)}{\partial t} \quad (2.10)$$

where

$$\alpha = \frac{k}{\rho C_p} \quad \text{is the thermal diffusivity} \quad (2.11)$$

Here, the thermal diffusivity α is a property of the medium and has dimensions of $length^2/time$, which may be given in the units m^2/hr or m^2/sec . The physical significance of thermal diffusivity is associated with the speed of propagation of heat into the solid during changes of temperature with time. The higher the thermal

diffusivity, the faster is the propagation of heat in the medium. The larger the thermal diffusivity, the shorter is the time required for the applied heat to penetrate into the depth of the solid.

For a medium with constant k , and no heat generation, equation (2.11) become

$$\nabla^2 T(\vec{r}, t) = \frac{1}{\alpha} \frac{\partial T(\vec{r}, t)}{\partial t} \quad (2.12)$$

The steady- state version of equation (2.12) is

$$\nabla^2 T(\vec{r}, t) = 0 \quad (2.13)$$

CHAPTER 3

COORDINATE SYSTEMS

3.1 INTRODUCTION

A Cartesian coordinate system offers the unique advantage that all three unit vectors, $\hat{\mathbf{i}}$, $\hat{\mathbf{j}}$, and $\hat{\mathbf{k}}$, are constants. Unfortunately, not all physical problems are well adapted to solution in Cartesian coordinates. Several problems are more readily solvable in other coordinates than if they were described in the Cartesian system. Generally, a coordinate system should be chosen to fit the problem under consideration in terms of symmetry and constraints. In this study, we describe and use the naturally-fit bispherical coordinates system.

3.2 ORTHOGONAL CURVILINEAR COORDINATES

In Cartesian coordinates we deal with three mutually perpendicular families of planes: $x = \text{constant}$, $y = \text{constant}$, and $z = \text{constant}$. We superimpose on this system three other families of surfaces. The surfaces of any one family need not be parallel to each other and they need not be planes. Any point is described as the intersection of three planes in Cartesian coordinates or as the intersection of the three surfaces which form curvilinear coordinates. Describing curvilinear coordinates surfaces by $u_1 = c_1$, $u_2 = c_2$, $u_3 = c_3$ where c_1, c_2 , and c_3 are constants, we identify a point by three numbers (u_1, u_2, u_3) , called the curvilinear coordinates of the point.

Let the functional relationship between curvilinear coordinates (u_1, u_2, u_3) and the Cartesian coordinates (x, y, z) be given as [32]

$$\begin{aligned} x &= x(u_1, u_2, u_3) \\ y &= y(u_1, u_2, u_3) \\ z &= z(u_1, u_2, u_3) \end{aligned} \quad (3.1)$$

which can be inverted as

$$\begin{aligned} u_1 &= u_1(x, y, z) \\ u_2 &= u_2(x, y, z) \\ u_3 &= u_3(x, y, z) \end{aligned} \quad (3.2)$$

Through any point P in the domain, having curvilinear coordinates (c_1, c_2, c_3) , there will pass three isotimic surfaces (a surface in space on which the value of a given quantity is everywhere equal; isotimic surfaces are the common reference surfaces for synoptic charts, principally constant-pressure surfaces and constant-height surfaces) $u_1(x, y, z) = c_1$, $u_2(x, y, z) = c_2$, $u_3(x, y, z) = c_3$. As illustrated in Figure 3.1, these surfaces intersect in pairs to give three curves passing through P , along each of which only one coordinate varies; these are the coordinate's curves.

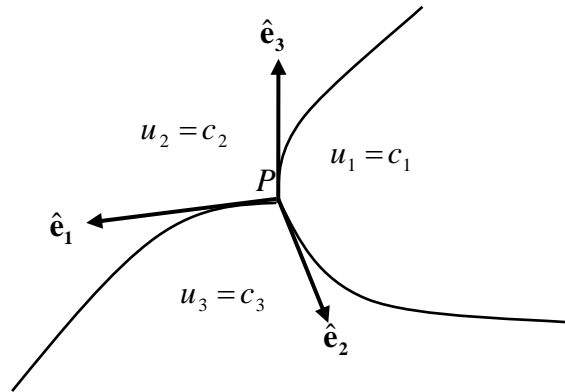


Figure 3.1. A curvilinear Coordinate System (u_1, u_2, u_3)

The normal to the surface $u_i = c_i$ is the gradient

$$\vec{\nabla}u_i = \frac{\partial u_i}{\partial x} \hat{\mathbf{i}} + \frac{\partial u_i}{\partial y} \hat{\mathbf{j}} + \frac{\partial u_i}{\partial z} \hat{\mathbf{k}} \quad (3.3)$$

The tangent to the coordinate curve for u_i is the vector

$$\frac{\partial \vec{r}}{\partial u_i} = \frac{\partial x}{\partial u_i} \hat{\mathbf{i}} + \frac{\partial y}{\partial u_i} \hat{\mathbf{j}} + \frac{\partial z}{\partial u_i} \hat{\mathbf{k}} \quad (3.4)$$

We say that u_1, u_2 , and u_3 are orthogonal curvilinear coordinates, whenever the vectors $\vec{\nabla}u_1, \vec{\nabla}u_2$ and $\vec{\nabla}u_3$ are mutually orthogonal at every point [32]. Each gradient vector $\vec{\nabla}u_i$ is parallel to the tangent vector $\frac{\partial \vec{r}}{\partial u_i}$ for the corresponding coordinate curve, and any coordinate curve for u_i intersects the isotimic surface $u_i = c_i$ at right angles when (u_1, u_2, u_3) form orthogonal curvilinear coordinates. To see this, consider a coordinate curve for u_1 .

- This curve is the intersection of two surfaces $u_2 = c_2$ and $u_3 = c_3$. Hence, its tangent $\frac{\partial \vec{r}}{\partial u_1}$ is perpendicular to both surface normals $\vec{\nabla}u_2$ and $\vec{\nabla}u_3$.
- The vector $\vec{\nabla}u_1$ is also perpendicular to $\vec{\nabla}u_2$ and $\vec{\nabla}u_3$.
- This implies that $\frac{\partial \vec{r}}{\partial u_1}$ is parallel to $\vec{\nabla}u_1$.

Since both of $\frac{\partial \vec{r}}{\partial u_1}$ and $\vec{\nabla}u_1$ point in the direction of increasing u_1 , they are parallel. It

follows, that the vectors $\frac{\partial \vec{r}}{\partial u_1}, \frac{\partial \vec{r}}{\partial u_2}$ and $\frac{\partial \vec{r}}{\partial u_3}$ form a right-handed system of mutually orthogonal vectors.

Define the right-handed system of mutually orthogonal unit vectors $(\hat{\mathbf{e}}_1, \hat{\mathbf{e}}_2, \hat{\mathbf{e}}_3)$ by

$$\hat{\mathbf{e}}_i = \frac{\frac{\partial \vec{r}}{\partial u_i}}{\left| \frac{\partial \vec{r}}{\partial u_i} \right|} \quad i = 1, 2, 3 \quad (3.5)$$

We need three functions h_i known as the scale factors to express the vector operations in orthogonal curvilinear coordinates. The scale factor h_i is defined to be the rate at which the arc length increases on the i th coordinate curve, with respect to u_i . In other words, if s_i denotes arc length on the i th coordinate curve measured in the direction of increasing u_i , then

$$h_i = \frac{ds_i}{du_i} \quad i = 1, 2, 3 \quad (3.6)$$

Since arc length can be expressed as

$$ds = |d\vec{r}| = \left| \frac{\partial \vec{r}}{\partial u_1} du_1 + \frac{\partial \vec{r}}{\partial u_2} du_2 + \frac{\partial \vec{r}}{\partial u_3} du_3 \right| \quad (3.7)$$

we see that

$$h_i = \left| \frac{\partial \vec{r}}{\partial u_i} \right| \quad i = 1, 2, 3 \quad (3.8)$$

Hence,

$$h_i^2 = \left(\frac{\partial x}{\partial u_i} \right)^2 + \left(\frac{\partial y}{\partial u_i} \right)^2 + \left(\frac{\partial z}{\partial u_i} \right)^2 \quad i = 1, 2, 3 \quad (3.9)$$

Combining equations (3.7) and (3.8) shows that the displacement vector can be expressed in terms of the scale factors by

$$d\vec{r} = h_1 du_1 \hat{e}_1 + h_2 du_2 \hat{e}_2 + h_3 du_3 \hat{e}_3 \quad (3.10)$$

A differential length (ds) in the rectangular coordinate system (x, y, z) is given by

$$(ds)^2 = (dx)^2 + (dy)^2 + (dz)^2 \quad (3.11)$$

The differentials dx , dy and dz are obtained from equation (3.1) by differentiation

$$dx = \frac{\partial x}{\partial u_1} du_1 + \frac{\partial x}{\partial u_2} du_2 + \frac{\partial x}{\partial u_3} du_3 \quad (3.12a)$$

$$dy = \frac{\partial y}{\partial u_1} du_1 + \frac{\partial y}{\partial u_2} du_2 + \frac{\partial y}{\partial u_3} du_3 \quad (3.12b)$$

$$dz = \frac{\partial z}{\partial u_1} du_1 + \frac{\partial z}{\partial u_2} du_2 + \frac{\partial z}{\partial u_3} du_3 \quad (3.12c)$$

Substitute equations (3.12) into equation (3.11), it becomes

$$(ds)^2 = d\vec{r} \cdot d\vec{r} = h_1^2 (du_1)^2 + h_2^2 (du_2)^2 + h_3^2 (du_3)^2 \quad (3.13)$$

In rectangular coordinates system, a differential volume element dV is given by

$$dV = dx dy dz \quad (3.14)$$

and the differential areas dA_x , dA_y and dA_z cut from the planes $x = \text{constant}$, $y = \text{constant}$, and $z = \text{constant}$ are given, respectively, by

$$dA_x = dy dz, \quad dA_y = dx dz, \quad dA_z = dx dy \quad (3.15)$$

In orthogonal curvilinear coordinates system, the elementary lengths from equation (3.6) are given by

$$ds_i = h_i du_i \quad i = 1, 2, 3 \quad (3.16)$$

Then, an elementary volume element dV in orthogonal curvilinear coordinates system takes the form

$$dV = h_1 h_2 h_3 du_1 du_2 du_3 \quad (3.17)$$

The differential areas dA_1 , dA_2 and dA_3 cut from the planes $u_1 = c_1$, $u_2 = c_2$ and $u_3 = c_3$ are given, respectively, by

$$\begin{aligned} dA_1 &= ds_2 ds_3 = h_2 h_3 du_2 du_3 \\ dA_2 &= ds_1 ds_3 = h_1 h_3 du_1 du_3 \\ dA_3 &= ds_1 ds_2 = h_1 h_2 du_1 du_2 \end{aligned} \quad (3.18)$$

The gradient is a vector having the magnitude and direction of the maximum space rate of change. Then, for any function $\psi(u_1, u_2, u_3)$ the component of $\vec{\nabla}\psi(u_1, u_2, u_3)$ in the \hat{e}_1 direction is given by

$$\vec{\nabla}\psi|_1 = \frac{d\psi}{ds_1} = \frac{\partial\psi}{h_1 \partial u_1} \quad (3.19)$$

It is the rate of change of ψ with respect to distance in the \hat{e}_1 direction. Since \hat{e}_1, \hat{e}_2 and \hat{e}_3 are mutually orthogonal unit vectors, the gradient becomes

$$\begin{aligned} \text{grad } \psi &= \vec{\nabla}\psi(u_1, u_2, u_3) = \frac{d\psi}{ds_1} \hat{e}_1 + \frac{d\psi}{ds_2} \hat{e}_2 + \frac{d\psi}{ds_3} \hat{e}_3 \\ &= \frac{1}{h_1} \frac{\partial\psi}{\partial u_1} \hat{e}_1 + \frac{1}{h_2} \frac{\partial\psi}{\partial u_2} \hat{e}_2 + \frac{1}{h_3} \frac{\partial\psi}{\partial u_3} \hat{e}_3 \end{aligned} \quad (3.20)$$

Let $\vec{F} = F_1 \hat{e}_1 + F_2 \hat{e}_2 + F_3 \hat{e}_3$ be a vector field, given in terms of the unit vectors \hat{e}_1, \hat{e}_2 and \hat{e}_3 . Then the divergence of \vec{F} , denoted $\text{div } \vec{F}$, or $\vec{\nabla} \cdot \vec{F}$ is given by [30]

$$\vec{\nabla} \cdot \vec{F}(u_1, u_2, u_3) = \lim_{\int dV \rightarrow 0} \frac{\int \vec{F} \cdot d\vec{\sigma}}{\int dV} \quad (3.21)$$

where $\int dV$ is the volume of a small region of space and $d\vec{\sigma}$ is the vector area element of this volume.

We shall compute the total flux of the field \vec{F} out of the small rectangular parallelepiped, Figure 3. 2. We, then, divide this flux by the volume of the box and take the limit as the dimensions of the box go to zero. This limit is the $\vec{\nabla} \cdot \vec{F}$. Note that the positive direction has been chosen so that (u_1, u_2, u_3) or $(\hat{e}_1, \hat{e}_2, \hat{e}_3)$ form a right-handed system.

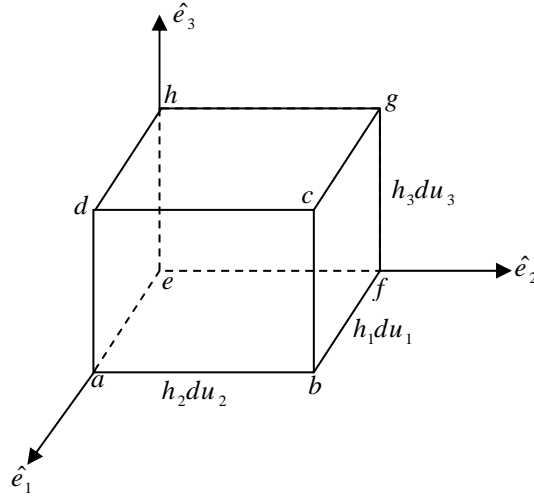


Figure 3. 2. Differential Rectangular Parallelepiped

The area of the face $abcd$ is $h_2 h_3 du_2 du_3$ and the flux normal is $\vec{F} \cdot \hat{e}_1 = F_1$. Then the flux outward from the face $abcd$ is $F_1 h_2 h_3 du_2 du_3$. The outward unit normal to the face $efgh$ is $-\hat{e}_1$, so its outward flux is $-F_1 h_2 h_3 du_2 du_3$. Since F_1, h_2 and h_3 are functions of u_1 as we move along the u_1 -coordinate curve, the sum of these two is approximately

$$\left[\frac{\partial}{\partial u_1} (F_1 h_2 h_3) du_1 \right] du_2 du_3 \quad (3.22)$$

Adding in the similar results for the other two pairs of faces; we obtain the net flux outward from the parallelepiped as

$$\left[\frac{\partial}{\partial u_1} (F_1 h_2 h_3) + \frac{\partial}{\partial u_2} (F_2 h_1 h_3) + \frac{\partial}{\partial u_3} (F_3 h_1 h_2) \right] du_1 du_2 du_3 \quad (3.23)$$

Divide equation (3.23) by the differential volume in equation (3.17). Hence the flux output per unit volume is given by

$$\text{div } \vec{F} = \vec{\nabla} \cdot \vec{F} = \frac{1}{h_1 h_2 h_3} \left[\frac{\partial}{\partial u_1} (F_1 h_2 h_3) + \frac{\partial}{\partial u_2} (F_2 h_1 h_3) + \frac{\partial}{\partial u_3} (F_3 h_1 h_2) \right] \quad (3.24)$$

Using equations (3.20) and (3.24), the Laplacian takes the form, given as

$$\nabla^2 \psi = \text{div grad } \psi$$

$$= \frac{1}{h_1 h_2 h_3} \left[\frac{\partial}{\partial u_1} \left(\frac{h_2 h_3}{h_1} \frac{\partial \psi}{\partial u_1} \right) + \frac{\partial}{\partial u_2} \left(\frac{h_1 h_3}{h_2} \frac{\partial \psi}{\partial u_2} \right) + \frac{\partial}{\partial u_3} \left(\frac{h_1 h_2}{h_3} \frac{\partial \psi}{\partial u_3} \right) \right] \quad (3.25)$$

By using equation (3.25), equations (2.12) and (2.13) can, respectively, written as

$$\frac{1}{h_1 h_2 h_3} \left[\frac{\partial}{\partial u_1} \left(\frac{h_2 h_3}{h_1} \frac{\partial T}{\partial u_1} \right) + \frac{\partial}{\partial u_2} \left(\frac{h_1 h_3}{h_2} \frac{\partial T}{\partial u_2} \right) + \frac{\partial}{\partial u_3} \left(\frac{h_1 h_2}{h_3} \frac{\partial T}{\partial u_3} \right) \right] = \frac{1}{\alpha} \frac{\partial T}{\partial t} \quad (3.26)$$

$$\frac{\partial}{\partial u_1} \left(\frac{h_2 h_3}{h_1} \frac{\partial T}{\partial u_1} \right) + \frac{\partial}{\partial u_2} \left(\frac{h_1 h_3}{h_2} \frac{\partial T}{\partial u_2} \right) + \frac{\partial}{\partial u_3} \left(\frac{h_1 h_2}{h_3} \frac{\partial T}{\partial u_3} \right) = 0 \quad (3.27)$$

These are, respectively, the transient and steady- states differential equations of heat conduction with no heat generation in a general orthogonal curvilinear coordinate system.

3.3 BISPHERICAL COORDINATE SYSTEM

The Bispherical Coordinates System (θ, ξ, φ) is a three-dimensional orthogonal coordinate system that results from rotating the two dimensional bipolar coordinate system about the axis that connects the two foci. The two foci located at $(0, 0, \pm a)$, under this rotation, remain as points in the bispherical coordinate system, [30, 33]

The transformation equations of the bispherical coordinates system are

$$x = \frac{a \sin \theta \cos \varphi}{\cosh \xi - \cos \theta}, y = \frac{a \sin \theta \sin \varphi}{\cosh \xi - \cos \theta} \text{ and } z = \frac{a \sinh \xi}{\cosh \xi - \cos \theta} \quad (3.28)$$

The coordinates surfaces are

a) Surfaces of constant ξ ($-\infty < \xi < \infty$) given by

$$x^2 + y^2 + (z - a \coth \xi)^2 = \frac{a^2}{\sinh^2 \xi} \quad (3.29)$$

which are non-intersecting spheres with centers at $(0, 0, a \coth \xi)$ and radii $\left| \frac{a}{\sinh \xi} \right|$ that surround the foci, Figure 3.3.

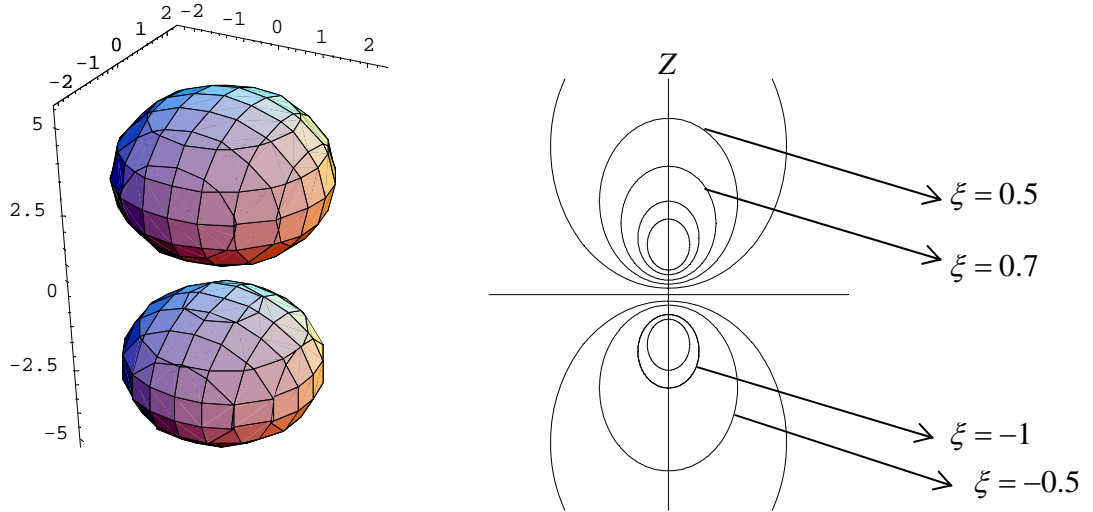


Figure 3.3. Surfaces of constant ξ

b) Surfaces of constant $\theta(0 \leq \theta \leq \pi)$ given by

$$x^2 + y^2 + z^2 - 2a\sqrt{x^2 + y^2} \cot \theta = a^2 \quad (3.30)$$

which look like apples when $(0 < \theta < \frac{\pi}{2})$, spheres when $(\theta = \frac{\pi}{2})$, and lemons

when $(\frac{\pi}{2} < \theta < \pi)$, Figure 3.4.

c) Surfaces of constant $\varphi(0 \leq \varphi < 2\pi)$ given by

$$\tan \varphi = \frac{y}{x} \quad (3.31)$$

which are half planes through the z-axis.

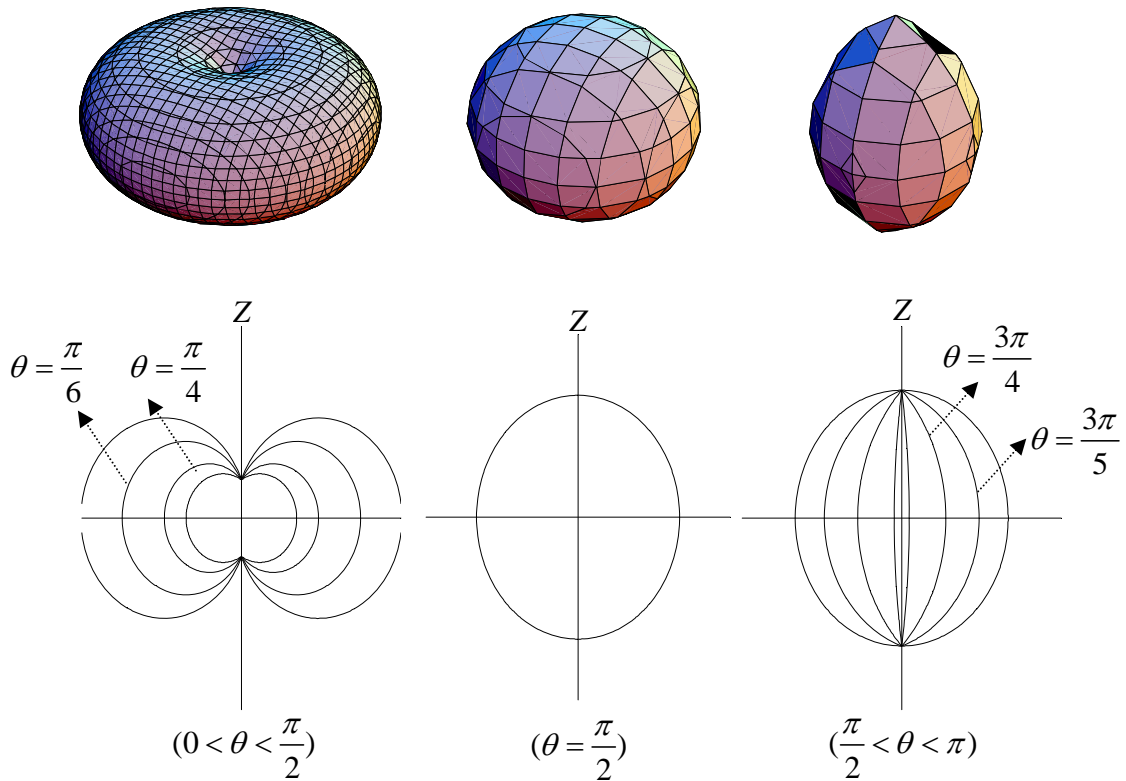


Figure 3.4. Surfaces of Constant θ

The bispherical coordinates system put together is sketched in Figure 3.5.

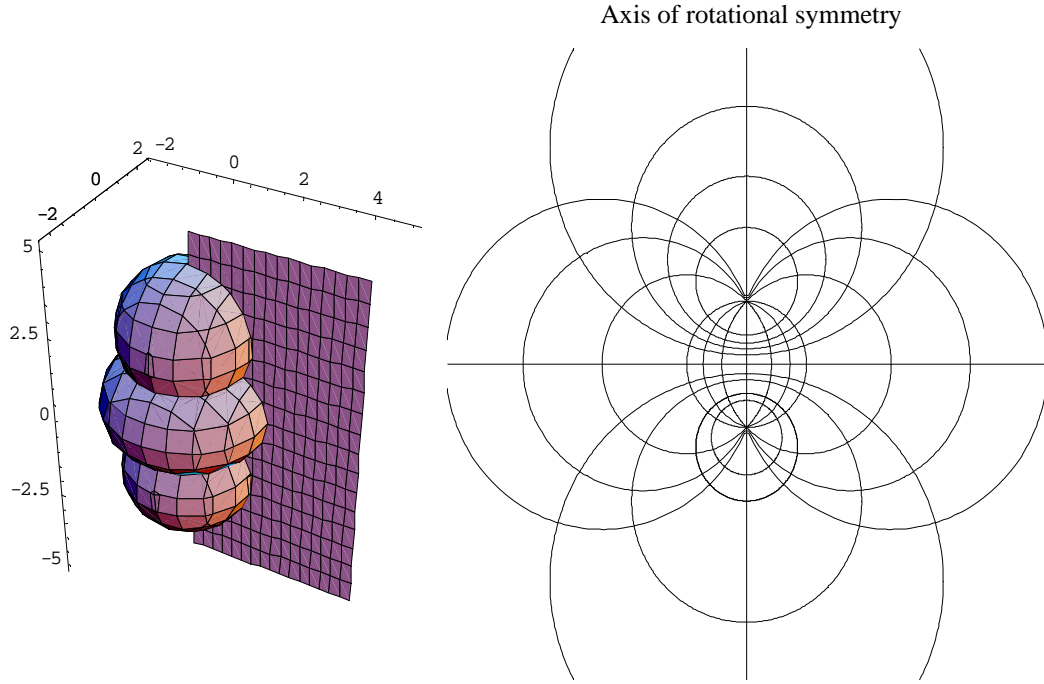


Figure 3.5. Bispherical coordinate system

It can be shown that specifying the radius of each of the two spheres (r_1 and r_2) and the center-to-center distance (H) fixes a particular bispherical coordinates system in the sense that $\xi = \xi_1 < 0$ (first sphere), $\xi = \xi_2 > 0$ (second sphere), and a are uniquely determined.

The radii of the two spheres are given by equation (3.29) as

$$r_1 = \left| \frac{a}{\sinh \xi_1} \right| \text{ and } r_2 = \left| \frac{a}{\sinh \xi_2} \right| \quad (3.32)$$

with centers on the z-axis given as $a \coth \xi_1$ and $a \coth \xi_2$.

Equation (3.32) can be rewritten as

$$\xi_1 = -\sinh^{-1} \frac{a}{r_1} \text{ and } \xi_2 = \sinh^{-1} \frac{a}{r_2} \quad (3.33)$$

The distance between the centers of the two spheres, H , is given by

$$H = a \coth \xi_2 - a \coth \xi_1 \quad (3.34)$$

By solving the system of equations (3.33) and (3.34) we can write a as

$$a = \frac{\sqrt{(H + r_1 + r_2)(H + r_1 - r_2)(H - r_1 - r_2)(H - r_1 + r_2)}}{2H} \quad (3.35)$$

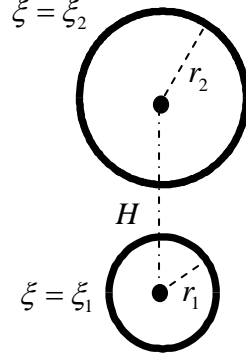


Figure 3.6. Distance between the centers of the spheres

The scale factors for the bispherical coordinates system are

$$h_1 = h_\theta = \frac{a}{\cosh \xi - \cos \theta} \quad (3.36a)$$

$$h_2 = h_\xi = \frac{a}{\cosh \xi - \cos \theta} \quad (3.36b)$$

$$h_3 = h_\phi = \frac{a \sin \theta}{\cosh \xi - \cos \theta} \quad (3.36c)$$

Substituting equations of the scale factors (3.36) in equation (3.27), the differential equation of steady heat conduction with no heat generation in bispherical coordinates system can be written as

$$\frac{\partial}{\partial \theta} \left(\frac{\sin \theta}{\cosh \xi - \cos \theta} \frac{\partial T}{\partial \theta} \right) + \frac{\partial}{\partial \xi} \left(\frac{\sin \theta}{\cosh \xi - \cos \theta} \frac{\partial T}{\partial \xi} \right) + \frac{1}{\sin \theta (\cosh \xi - \cos \theta)} \frac{\partial^2 T}{\partial \phi^2} = 0 \quad (3.37)$$

CHAPTER 4

PROBLEM OF HEAT CONDUCTION FROM TWO ADJACENT SPHERES

4.1 PROBLEM STATEMENT

The problem considered here is that of two isothermal spheres, possibly of different diameters and different temperatures, placed in an infinite fluid at some distance from each other. The temperature of the first sphere ($\xi = \xi_1 < 0$) is maintained at T_1 , while the temperature of the second sphere ($\xi = \xi_2 > 0$) is maintained at T_2 . The temperature far away from the two spheres is denoted by T_∞ , Figure 4.1.

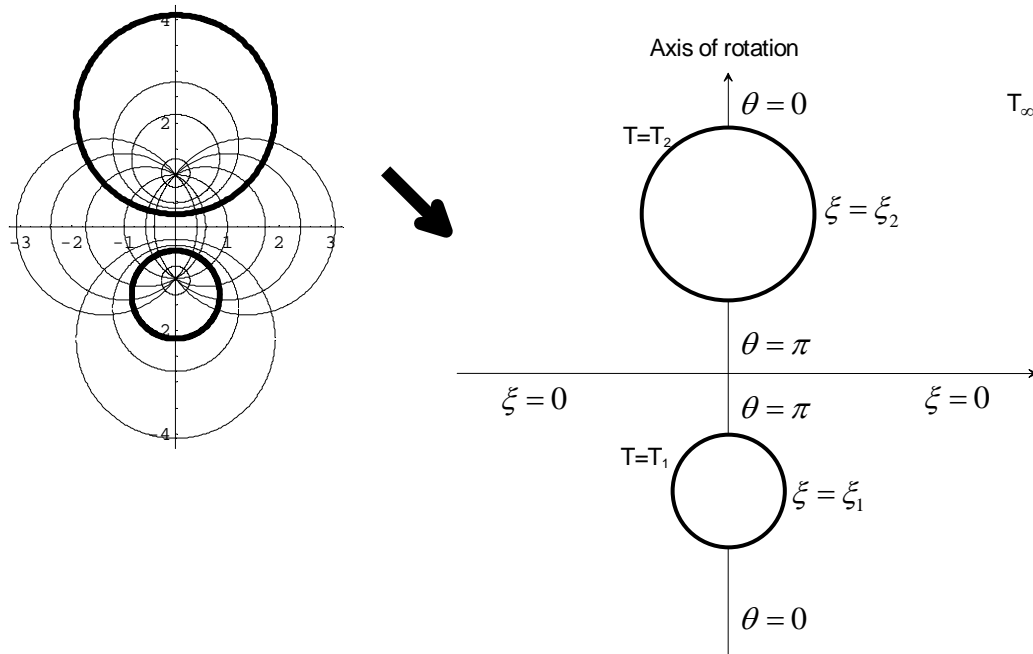


Figure 4.1. Problem configuration

4.2 ANALYTICAL STEADY-STATE SOLUTION

Since the problem is axisymmetric in φ (independent of φ), equation (3.37) reduces to

$$\frac{\partial}{\partial \theta} \left(\frac{\sin \theta}{\cosh \xi - \cos \theta} \frac{\partial T}{\partial \theta} \right) + \frac{\partial}{\partial \xi} \left(\frac{\sin \theta}{\cosh \xi - \cos \theta} \frac{\partial T}{\partial \xi} \right) = 0 \quad (4.1)$$

Along $\theta = 0$ or $\theta = \pi$, we expect no variation of temperature with respect to the direction θ . We may then write $\left. \frac{\partial T}{\partial \theta} \right|_{\theta=0} = 0$ and $\left. \frac{\partial T}{\partial \theta} \right|_{\theta=\pi} = 0$. Far away from the spheres,

the temperature is T_∞ . It is very important to recognize that the far field is represented in bispherical coordinates by the single point $(\theta, \xi, \varphi) \rightarrow (0, 0, \varphi)$. This single point represents the "huge sphere" with infinite radius that engulfs the whole domain. From this point onwards, we will drop the direction φ since the problem is axisymmetric. For example, we will refer to the far field as $(\theta, \xi) \rightarrow (0, 0)$ with the understanding that we actually mean $(\theta, \xi, \varphi) \rightarrow (0, 0, \varphi)$. The rectangular map of the region for the problem is shown in Figure 4.2.

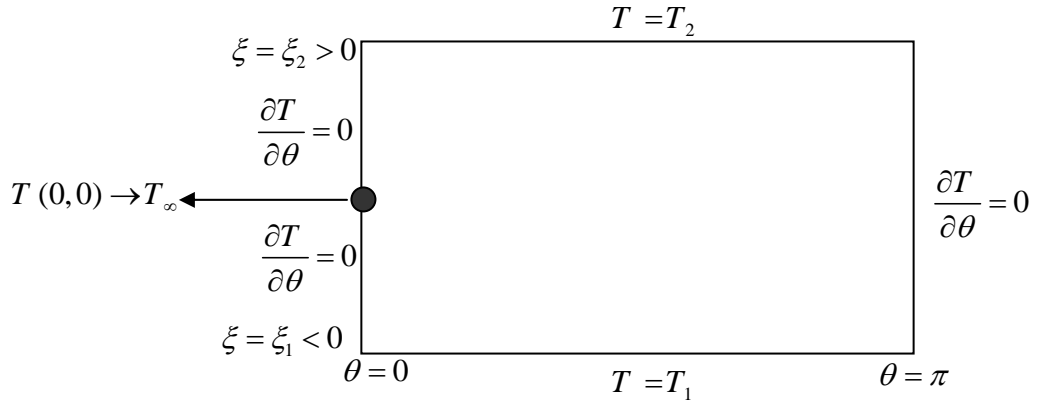


Figure 4.2. Rectangular region for the problem

It is well established tradition in fluid and thermal sciences to express the governing equations in dimensionless forms. The non-dimensional form of the equations helps to eliminate several physical constraints such as the use of particular units of measurements. We define the dimensionless temperature (U) as

$$U = \frac{T - T_\infty}{T_1 - T_\infty} \quad (4.2)$$

Accordingly, equation (4.1) can be rewritten in terms of the dimensionless temperature as

$$\frac{\partial}{\partial \theta} \left(\frac{\sin \theta}{\cosh \xi - \cos \theta} \frac{\partial U}{\partial \theta} \right) + \sin \theta \frac{\partial}{\partial \xi} \left(\frac{1}{\cosh \xi - \cos \theta} \frac{\partial U}{\partial \xi} \right) = 0 \quad (4.3)$$

The rectangular map of the region for the problem now looks like Figure 4.3. Note that when $T = T_1$, $U = 1$, and when $T = T_2$, $U = \frac{T_2 - T_\infty}{T_1 - T_\infty} = U_2$.

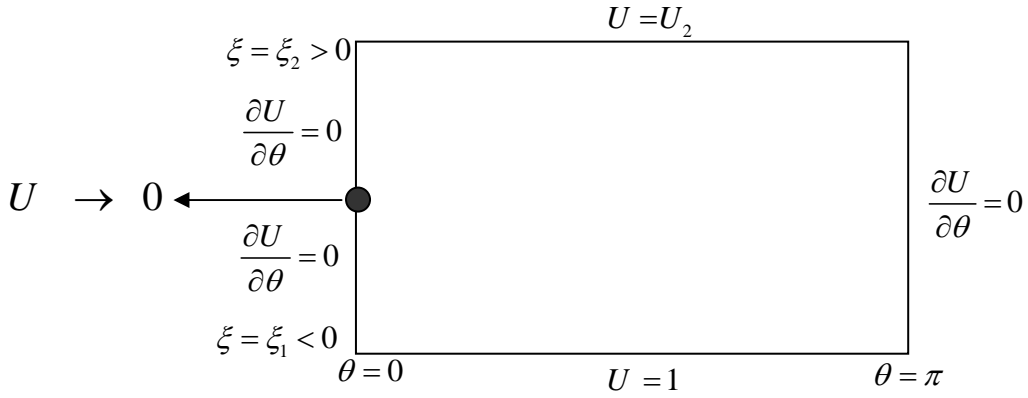


Figure 4.3. Rectangular region for the problem with dimensionless boundary conditions

The reader may wish to try and realize that equation (4.3) is not separable in the classical sense. The bispherical coordinate system is R-separation instead, [33]. A solution $\psi(x_1, x_2, x_3)$ of a differential equation in three variables is R-separable if it can be written in the form $\psi(x_1, x_2, x_3) = R(x_1, x_2, x_3)A(x_1)B(x_2)C(x_3)$ where $R(x_1, x_2, x_3)$ contains no factors that are functions of one variable. $R(x_1, x_2, x_3)$ is called the modulation factor because it modifies all factored solutions in the same way, [30]. Equation (4.3) admits the separation form [33]

$$U = \sqrt{\cosh \xi - \cos \theta} X(\theta) Z(\xi) \quad (4.4)$$

Equation (4.3) then reduces to

$$\frac{\cos(\theta) X'(\theta) + \sin(\theta) X''(\theta)}{\sin(\theta) X(\theta)} = \frac{Z(\xi) - 4Z''(\xi)}{4Z(\xi)} \quad (4.5)$$

In equation (4.5), the left-hand side is a function of the variable θ alone, and the right-hand side is a function of the variable ξ alone; the only way this equality can hold if

both sides are equal to the same constant, says $-\lambda$. Thus, the two separated solutions for the functions $X(\theta)$ and $Z(\xi)$ become

$$\sin(\theta)X''(\theta) + \cos(\theta)X'(\theta) + \lambda \sin(\theta)X(\theta) = 0 \quad (4.6)$$

$$Z''(\xi) - \left(\frac{1}{4} + \lambda\right)Z(\xi) = 0 \quad (4.7)$$

Let $w = \cos \theta$. Equation (4.6) can be written as

$$(1-w^2)\frac{d^2X}{dw^2} - 2w\frac{dX}{dw} + \lambda X = 0, \quad -1 < w < 1, \quad X \text{ is bounded as } w \rightarrow \pm 1. \quad (4.8)$$

We let $X = \sum_{i=0}^{\infty} c_i w^i$ and plug into equation (4.8). The result is, [35]

$$[2c_2 + \lambda c_0] + [(\lambda - 2)c_1 + 6c_3]w + \sum_{i=2}^{\infty} [(i+2)(i+1)c_{i+2} + (\lambda - i^2 - i)c_i]w^i = 0 \quad (4.9)$$

So we have c_0, c_1 arbitrary and

$$c_2 = \frac{-\lambda}{2}c_0 \quad (4.10)$$

$$c_3 = \frac{2-\lambda}{6}c_1 \quad (4.11)$$

and the recurrence relation is

$$c_{i+2} = \frac{i(i+1) - \lambda}{(i+1)(i+2)}c_i, \quad i = 2, 3, 4, \dots \quad (4.12)$$

Now, we want solutions that are bounded at $w = \pm 1$. However, if we look at

$$\lim_{i \rightarrow \infty} \frac{c_{i+2}}{c_i} = \lim_{i \rightarrow \infty} \frac{i(i+1) - \lambda}{(i+1)(i+2)} = 1 \quad (4.13)$$

we see that if $c_0 \neq 0$, we get an infinite series of even powers of w , which behaves like

the geometric series $\sum_{i=0}^{\infty} w^{2i}$. Similarly, $c_1 \neq 0$ gives us a series which behaves like

$\sum_{i=0}^{\infty} w^{2i+1}$. Each of these series diverges at $w = \pm 1$ and is unbounded at $w = 1$. So the

only way that we can have a bounded solution is if the series terminates, that is, if it is a polynomial. When will this happen?

Suppose $\lambda = n(n+1)$, where n is a positive integer. Then,

$$c_{n+2} = \frac{n(n+1) - n(n+1)}{(n+1)(n+2)} c_n = 0 \quad (4.14)$$

In this case, we will have

$$c_{n+2} = c_{n+4} = \dots = 0, \quad (4.15)$$

i.e., if n is odd, the series of odd powers will be a polynomial; similarly for n even. In each case, the other half of the series will still be infinite, the only way to eliminate it will be to choose $c_0 = 0$ or $c_1 = 0$, respectively.

Essentially, we have found that the numbers

$$\lambda_n = n(n+1), \quad n = 0, 1, 2, 3, 4, \dots \quad (4.16)$$

are the eigenvalues of the given boundary-value problem (4.8), while the eigenfunctions are the corresponding polynomial solutions.

with $\lambda = n(n+1)$, equation (4.8) becomes

$$(1-w^2) \frac{d^2 X}{dw^2} - 2w \frac{dX}{dw} + n(n+1)X = 0 \quad (4.17)$$

It is called Legendre's differential equation, and its solution is [30]

$$\begin{aligned} X &= \alpha_1 P_n(w) + \alpha_2 Q_n(w) \\ X &= \alpha_1 P_n(\cos \theta) + \alpha_2 Q_n(\cos \theta) \end{aligned} \quad (4.18)$$

where $P_n(w)$ and $Q_n(w)$ are called Legendre functions of degree n , of the first and the second kinds, respectively.

As the Q_n functions have logarithmic singularities at $\theta = \pm\pi$, for all values of n , we must have $\alpha_2 = 0$, then

$$X = \alpha_1 P_n(\cos \theta) \quad (4.19)$$

With $\lambda = n(n+1)$, equation (4.7) become

$$\begin{aligned} Z''(\xi) - \left(\frac{1}{4} + n(n+1)\right)Z(\xi) &= 0 \\ Z''(\xi) - \left(\frac{1}{4} + n^2 + n\right)Z(\xi) &= 0 \\ Z''(\xi) - \left(n + \frac{1}{2}\right)^2 Z(\xi) &= 0 \end{aligned} \quad (4.20)$$

and its solution is

$$Z(\xi) = \alpha_3 e^{(n+\frac{1}{2})\xi} + \alpha_4 e^{-(n+\frac{1}{2})\xi} \quad (4.21)$$

Using equations (4.19) and (4.21) in equation (4.3) gives the solution of steady-state conditions equation (4.3) as

$$U = \sqrt{\cosh \xi - \cos \theta} \sum_{n=0}^{\infty} (A_n e^{(n+\frac{1}{2})\xi} + B_n e^{-(n+\frac{1}{2})\xi}) P_n(\cos \theta) \quad (4.22)$$

Applying the top and bottom boundary conditions of Figure 4.3 to equation (4.22), we get

$$\frac{1}{\sqrt{\cosh \xi_1 - \cos \theta}} = \sum_{n=0}^{\infty} (A_n e^{(n+\frac{1}{2})\xi_1} + B_n e^{-(n+\frac{1}{2})\xi_1}) P_n(\cos \theta) \quad (4.23)$$

and

$$\frac{U_2}{\sqrt{\cosh \xi_2 - \cos \theta}} = \sum_{n=0}^{\infty} (A_n e^{(n+\frac{1}{2})\xi_2} + B_n e^{-(n+\frac{1}{2})\xi_2}) P_n(\cos \theta) \quad (4.24)$$

From the generating function of Legendre polynomials [30]

$$g(t, x) = (1 - 2xt + t^2)^{-\frac{1}{2}} = \sum_{n=0}^{\infty} P_n(x) t^n, \quad |t| < 1 \quad (4.25)$$

obtain, with $t = e^{\pm \xi}$ and $x = \cos \theta$

$$\frac{1}{\sqrt{\cosh \xi - \cos \theta}} = \sqrt{2} \sum_{n=0}^{\infty} P_n(\cos \theta) e^{-(n+\frac{1}{2})|\xi|} \quad (4.26)$$

Comparing equation (4.26) to equations (4.23) and (4.24), we get two equations for the constants A_n and B_n

$$\sqrt{2} e^{(n+\frac{1}{2})\xi_1} = A_n e^{(n+\frac{1}{2})\xi_1} + B_n e^{-(n+\frac{1}{2})\xi_1} \quad (4.27)$$

$$\sqrt{2} U_2 e^{-(n+\frac{1}{2})\xi_2} = A_n e^{(n+\frac{1}{2})\xi_2} + B_n e^{-(n+\frac{1}{2})\xi_2} \quad (4.28)$$

It follows that

$$A_n = \frac{\sqrt{2} (e^{(1+2n)\xi_1} - U_2)}{e^{(1+2n)\xi_1} - e^{(1+2n)\xi_2}} \quad (4.29)$$

$$B_n = \frac{\sqrt{2} e^{(1+2n)\xi_1} (U_2 - e^{(1+2n)\xi_2})}{e^{(1+2n)\xi_1} - e^{(1+2n)\xi_2}} \quad (4.30)$$

Substituting equations (4.29) and (4.30) in equation (4.22), the solution can be written as

$$U = \sqrt{\cosh \xi - \cos \theta} \sum_{n=0}^{\infty} \left(\frac{\sqrt{2} (e^{(1+2n)\xi_1} - U_2)}{e^{(1+2n)\xi_1} - e^{(1+2n)\xi_2}} e^{(n+\frac{1}{2})\xi} + \frac{\sqrt{2} e^{(1+2n)\xi_1} (U_2 - e^{(1+2n)\xi_2})}{e^{(1+2n)\xi_1} - e^{(1+2n)\xi_2}} e^{-(n+\frac{1}{2})\xi} \right) P_n(\cos \theta) \quad (4.31)$$

Figure 4.4 shows the isotherms of a typical solution (the case $r_1 = 1, r_2 = 3, H = 5$, and $U_2 = 2$).

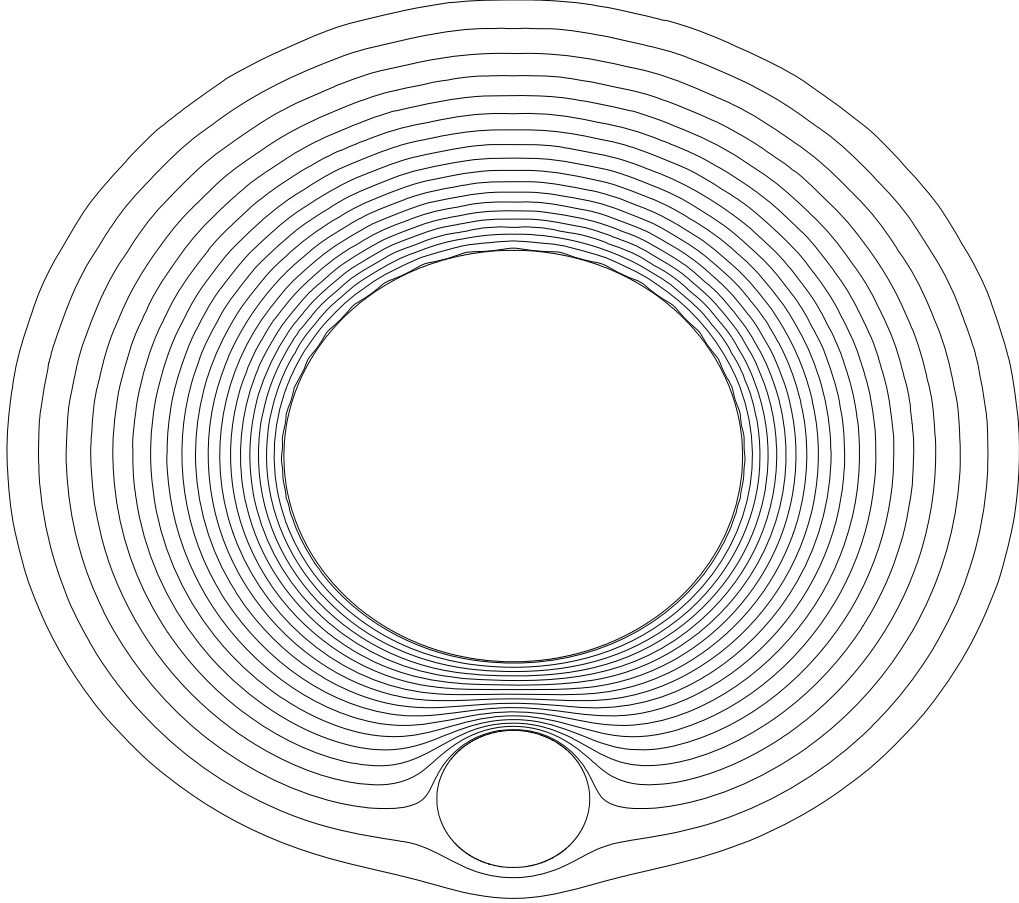


Figure 4.4. Isotherms of the case $r_1 = 1, r_2 = 3, H = 5$, and $U_2 = 2.0$

Isotherms shown are: 2.0, 1.94, 1.88, ..., 0.9

4.3 RATE OF HEAT TRANSFER

The local rate of heat transferred from any of the two spheres is

$$q(\theta) = -k \left(\frac{1}{h_\xi} \frac{\partial T}{\partial \xi} \right)_{\xi=\xi^*} \quad (4.32)$$

By using $U = \frac{T - T_\infty}{T_1 - T_\infty}$,

$$q(\theta) = -\frac{k}{h_\xi} \left[(T_1 - T_\infty) \frac{\partial U}{\partial \xi} \right]_{\xi=\xi^*} \quad (4.33)$$

where k is the thermal conductivity, h_ξ is the scale factor of the coordinate system and

is given by $h_\xi = \frac{a}{\cosh \xi - \cos \theta}$, and ξ^* may be either ξ_1 or ξ_2 .

The local Nusselt number (N_u) is defined as

$$N_u(\theta) = \frac{2r_1 q(\theta)}{k(T_1 - T_\infty)} = -2r_1 \left(\frac{1}{h_\xi} \frac{\partial U}{\partial \xi} \right)_{\xi=\xi^*} \quad (4.34)$$

In equation (4.34), we chose to scale by the diameter of the lower sphere. We fix the radius of the lower sphere at a value of unity. Its scaled temperature is also fixed at unity. We do not lose generality by fixing such values since the relative sizes of the spheres can be controlled by choosing an appropriate size of the top sphere as to obtain the desired size relative to the fixed-size lower sphere. By the same argument, given two spheres with two different temperatures, we numerate the spheres (rotate the coordinates system up-side-down if necessary) appropriately and use equation (4.34) for scaling. The case when the two spheres are at the same temperature as the far field temperature is trivial. Equation (4.34) with $r_1 = 1$ can now be written as

$$N_u(\theta) = -2 \left[\frac{(\cosh \xi - \cos \theta)}{a} \frac{\partial U}{\partial \xi} \right]_{\xi=\xi^*} \quad (4.35)$$

So for the reasons mentioned above, we will only calculate the heat transfer coefficient on the top sphere (ξ_2). By using equation (4.31), the following is an explicit expression of the local Nusselt number at the top sphere.

$$N_u(\theta) = -\frac{2}{a} \left\{ \frac{\sinh \xi_2}{2} (\cosh \xi_2 - \cos \theta)^{\frac{1}{2}} \sum_{n=0}^{\infty} \left[A_n e^{(n+\frac{1}{2})\xi_2} + B_n e^{-(n+\frac{1}{2})\xi_2} \right] P_n(\cos \theta) + \right. \\ \left. (\cosh \xi_2 - \cos \theta)^{\frac{3}{2}} \sum_{n=0}^{\infty} \left[A_n \left(n + \frac{1}{2}\right) e^{(n+\frac{1}{2})\xi_2} - \left(n + \frac{1}{2}\right) B_n e^{-(n+\frac{1}{2})\xi_2} \right] P_n(\cos \theta) \right\} \quad (4.36)$$

Averaging the Nusselt number over the surface of a sphere gives the average Nusselt number, $\overline{N_u}$, as

$$\overline{N_u} = \frac{\int_{\sigma} N_u(\theta) dA}{\int_{\sigma} dA} \quad (4.37)$$

On the top sphere (ξ_2)

$$\int_{\sigma} dA = A = \frac{4\pi a^2}{\sinh^2 \xi_2} \quad (4.38)$$

If we take a patch from the surface area of the top sphere (ξ_2), then Figure 4.5 shows that the two edges of the patch that meet at the same point can be approximated by the vectors $\frac{\partial \vec{r}}{\partial \theta}$ and $\frac{\partial \vec{r}}{\partial \phi}$. Then,

$$dA = \left| \frac{\partial \vec{r}}{\partial \theta} \times \frac{\partial \vec{r}}{\partial \phi} \right| d\theta d\phi = \frac{a^2 \sin \theta}{(\cosh \xi_2 - \cos \theta)^2} d\theta d\phi \quad (4.39)$$

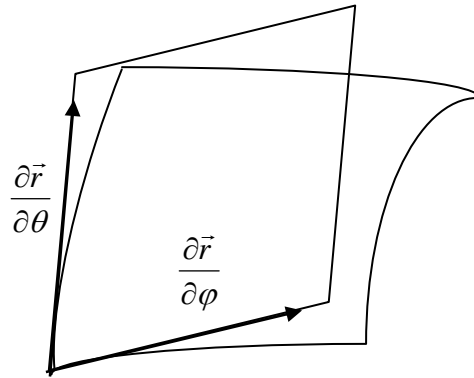


Figure 4.5. Approximating a patch by a parallelogram

By using equations (4.36) and (4.39) and integrating over θ ($0 \leq \theta \leq \pi$), we get

$$\begin{aligned} \int_{\sigma} N_u(\theta) dA = & \\ -2a\pi \sinh \xi_2 \sum_{n=0}^{\infty} \left[A_n e^{\left(\frac{1}{2}+n\right)\xi_2} + B_n e^{-\left(\frac{1}{2}+n\right)\xi_2} \right] \int_0^{\pi} (\cosh \xi_2 - \cos \theta)^{-\frac{3}{2}} P_n(\cos \theta) \sin \theta d\theta & \\ -4a\pi \sum_{n=0}^{\infty} \left[\left(\frac{1}{2}+n\right) A_n e^{\left(\frac{1}{2}+n\right)\xi_2} - \left(\frac{1}{2}+n\right) B_n e^{-\left(\frac{1}{2}+n\right)\xi_2} \right] \int_0^{\pi} (\cosh \xi_2 - \cos \theta)^{-\frac{1}{2}} P_n(\cos \theta) \sin \theta d\theta & \end{aligned} \quad (4.40)$$

From the Table of Integrals [34], we can find directly that

$$\int_0^{\pi} (\cosh \xi_2 - \cos \theta)^{-\frac{1}{2}} P_n(\cos \theta) \sin \theta d\theta = \frac{2\sqrt{2}}{2n+1} e^{-\left(\frac{1}{2}+n\right)\xi_2} \quad (4.41)$$

For $\int_0^{\pi} (\cosh \xi_2 - \cos \theta)^{-3/2} \sin \theta P_n(\cos \theta) d\theta$, we use the substitution $z = \cos \theta$. Then

$$\int_0^{\pi} (\cosh \xi_2 - \cos \theta)^{-3/2} \sin \theta P_n(\cos \theta) d\theta = \int_{-1}^1 (\cosh \xi_2 - z)^{-3/2} P_n(z) dz \quad (4.42)$$

We make use of the standard result [34],

$$\frac{1}{2} \Gamma(1+\mu) \int_{-1}^1 P_n(z) (\omega - z)^{-\mu-1} dz = (\omega^2 - 1)^{-\mu/2} e^{-i\pi\mu} Q_n^{\mu}(\omega) \quad (4.43)$$

where Γ is the Gamma function, Q_n^{μ} is the associated Legendre polynomials of the

second kind. With $\mu = \frac{1}{2}$ equation (4.43) yields

$$\int_{-1}^1 (\omega - z)^{-\frac{3}{2}} P_n(z) dz = \frac{2}{\Gamma(\frac{3}{2})} (\omega^2 - 1)^{-\frac{1}{4}} e^{-\frac{i\pi}{2}} Q_n^{\frac{1}{2}}(\omega) \quad (4.44)$$

It is possible to represent associated Legendre functions Q_n^{μ} of the second kind in the

form of a series by expressing them in terms of a Hypergeometric function (${}_2F_1$) as

$$Q_n^{\mu}(\omega) = \frac{e^{\mu\pi i} \Gamma(n+\mu+1) \Gamma(\frac{1}{2})}{2^{n+1} \Gamma(n+\frac{3}{2})} (\omega^2 - 1)^{\frac{\mu}{2}} \omega^{-n-\mu-1} {}_2F_1\left(\frac{n+\mu}{2}+1, \frac{n+\mu+1}{2}; n+\frac{3}{2}; \frac{1}{\omega^2}\right) \quad (4.45)$$

with $\mu = 1/2$ equation (4.45) yields

$$Q_n^{\frac{1}{2}}(\omega) = \frac{e^{\frac{\pi i}{2}} \Gamma(\frac{1}{2})}{2^{n+1}} (\omega^2 - 1)^{\frac{1}{4}} \omega^{-n-\frac{3}{2}} {}_2F_1\left(\frac{n}{2}+\frac{5}{4}, \frac{n}{2}+\frac{3}{4}; n+\frac{3}{2}; \frac{1}{\omega^2}\right) \quad (4.46)$$

Substitute equation (4.46) in equation (4.44), we get

$$\int_{-1}^1 (\omega - z)^{-\frac{3}{2}} P_n(z) dz = \frac{\omega^{-n-\frac{3}{2}}}{2^{n-1}} {}_2F_1\left(\frac{n}{2} + \frac{5}{4}, \frac{n}{2} + \frac{3}{4}; n + \frac{3}{2}; \frac{1}{\omega^2}\right) \quad (4.47)$$

By using the transformation formula

$$\begin{aligned} {}_2F_1(\alpha, \beta; \gamma; z) &= (1-z)^{-\alpha} \frac{\Gamma(\gamma)\Gamma(\beta-\alpha)}{\Gamma(\beta)\Gamma(\gamma-\alpha)} {}_2F_1\left(\alpha, \gamma-\beta; \alpha-\beta+1; \frac{1}{1-z}\right) \\ &\quad + (1-z)^{-\beta} \frac{\Gamma(\gamma)\Gamma(\alpha-\beta)}{\Gamma(\alpha)\Gamma(\gamma-\beta)} {}_2F_1\left(\beta, \gamma-\alpha; \beta-\alpha+1; \frac{1}{1-z}\right) \end{aligned} \quad (4.48)$$

The result (4.48) with $\alpha = \frac{n}{2} + \frac{5}{4}, \beta = \frac{n}{2} + \frac{3}{4}, \gamma = n + \frac{3}{2}$ and $z = \frac{1}{\omega^2}$ gives

$$\begin{aligned} {}_2F_1\left(\frac{n}{2} + \frac{5}{4}, \frac{n}{2} + \frac{3}{4}; n + \frac{3}{2}; \frac{1}{\omega^2}\right) &= \left(1 - \frac{1}{\omega^2}\right)^{-\left(\frac{n+5}{2}\right)} \frac{\Gamma\left(n + \frac{3}{2}\right)\Gamma\left(-\frac{1}{2}\right)}{\Gamma\left(\frac{n}{2} + \frac{3}{4}\right)\Gamma\left(\frac{n}{2} + \frac{1}{4}\right)} {}_2F_1\left(\frac{n}{2} + \frac{5}{4}, \frac{n}{2} + \frac{3}{4}; \frac{3}{2}; \frac{1}{1 - \frac{1}{\omega^2}}\right) \\ &\quad + \left(1 - \frac{1}{\omega^2}\right)^{-\left(\frac{n+3}{2}\right)} \frac{\Gamma\left(n + \frac{3}{2}\right)\Gamma\left(\frac{1}{2}\right)}{\Gamma\left(\frac{n}{2} + \frac{5}{4}\right)\Gamma\left(\frac{n}{2} + \frac{3}{4}\right)} {}_2F_1\left(\frac{n}{2} + \frac{3}{4}, \frac{n}{2} + \frac{1}{4}; \frac{1}{2}; \frac{1}{1 - \frac{1}{\omega^2}}\right) \end{aligned} \quad (4.49)$$

Using the doubling formula for gamma functions

$$\Gamma(2n) = \frac{2^{2n-1}}{\sqrt{\pi}} \Gamma(n) \Gamma\left(n + \frac{1}{2}\right) \quad (4.50)$$

and the fact that

$$\Gamma\left(\frac{1}{2}\right) = \sqrt{\pi} \quad \text{and} \quad \Gamma\left(-\frac{1}{2}\right) = -2\sqrt{\pi} \quad (4.51)$$

we can write (4.49) as

$$\begin{aligned} {}_2F_1\left(\frac{n}{2} + \frac{5}{4}, \frac{n}{2} + \frac{3}{4}; n + \frac{3}{2}; \frac{1}{\omega^2}\right) &= -2^{\frac{n+3}{2}} \left(\frac{n}{2} + \frac{1}{4}\right) \left(1 - \frac{1}{\omega^2}\right)^{-\left(\frac{n+5}{2}\right)} {}_2F_1\left(\frac{n}{2} + \frac{5}{4}, \frac{n}{2} + \frac{3}{4}; \frac{3}{2}; \frac{1}{1 - \frac{1}{\omega^2}}\right) \\ &\quad + 2^{\frac{n+1}{2}} \left(1 - \frac{1}{\omega^2}\right)^{-\left(\frac{n+3}{2}\right)} {}_2F_1\left(\frac{n}{2} + \frac{3}{4}, \frac{n}{2} + \frac{1}{4}; \frac{1}{2}; \frac{1}{1 - \frac{1}{\omega^2}}\right) \end{aligned} \quad (4.52)$$

The two hypergeometric functions in (4.52) have the following expressions [34]

$${}_2F_1\left(\frac{n}{2} + \frac{5}{4}, \frac{n}{2} + \frac{3}{4}; \frac{3}{2}; \chi\right) = (1-\chi)^{-n-\frac{1}{2}} \frac{(1+\sqrt{\chi})^{n+\frac{1}{2}} - (1-\sqrt{\chi})^{n+\frac{1}{2}}}{(1+2n)\sqrt{\chi}} \quad (4.53)$$

$${}_2F_1\left(\frac{n}{2} + \frac{3}{4}, \frac{n}{2} + \frac{1}{4}; \frac{1}{2}; \chi\right) = (1-\chi)^{-n-\frac{1}{2}} \frac{(1+\sqrt{\chi})^{n+\frac{1}{2}} - (1-\sqrt{\chi})^{n+\frac{1}{2}}}{2} \quad (4.54)$$

The result (4.52) can be written as

$${}_2F_1\left(\frac{n}{2} + \frac{5}{4}, \frac{n}{2} + \frac{3}{4}; n + \frac{3}{2}; \frac{1}{\omega^2}\right) = 2^{n+\frac{1}{2}} \left(1 - \frac{1}{\omega^2}\right)^{-\left(\frac{n+3}{2+4}\right)} \left(1 + \frac{1}{\sqrt{1 - \frac{1}{\omega^2}}}\right)^{-(n+\frac{1}{2})} \quad (4.55)$$

Substituting equation (4.55) in equation (4.47) yields

$$\int_{-1}^1 (\omega - z)^{-\frac{3}{2}} P_n(z) dz = 2\sqrt{2} \omega^{-(n+\frac{3}{2})} \left(1 - \frac{1}{\omega^2}\right)^{-\left(\frac{n+3}{2+4}\right)} \left(1 + \frac{1}{\sqrt{1 - \frac{1}{\omega^2}}}\right)^{-(n+\frac{1}{2})} \quad (4.56)$$

Equation (4.56) with $\omega = \cosh \xi_2$ ($\xi_2 > 0$) can be written as

$$\begin{aligned} \int_{-1}^1 (\omega - z)^{-\frac{3}{2}} P_n(z) dz &= 2\sqrt{2} (\cosh \xi_2)^{-(n+\frac{3}{2})} (1 - \operatorname{sech}^2 \xi_2)^{-\left(\frac{n+3}{2+4}\right)} \left(1 + \frac{1}{\tanh \xi_2}\right)^{-(n+\frac{1}{2})} \\ &= 2\sqrt{2} (\cosh \xi_2)^{-(n+\frac{3}{2})} (\tanh \xi_2)^{-(n+\frac{3}{2})} (1 + \coth \xi_2)^{-(n+\frac{1}{2})} \\ &= 2\sqrt{2} (\sinh \xi_2)^{-(n+\frac{3}{2})} (1 + \coth \xi_2)^{-(n+\frac{1}{2})} \\ &= \frac{2\sqrt{2}}{\sinh \xi_2} (\sinh \xi_2 + \cosh \xi_2)^{-(n+\frac{1}{2})} \\ &= \frac{2\sqrt{2}}{\sinh \xi_2} e^{-(n+\frac{1}{2})\xi_2} \end{aligned} \quad (4.57)$$

Hence

$$\int_0^\pi (\cosh \xi_2 - \cos \theta)^{-\frac{3}{2}} P_n(\cos \theta) \sin \theta d\theta = \frac{2\sqrt{2}}{\sinh \xi_2} e^{-(n+\frac{1}{2})\xi_2} \quad (4.58)$$

Using equations (4.41) and (4.58) in equation (4.40), we can write

$$\begin{aligned} \int_{\sigma} N_u(\theta) dA &= -4\sqrt{2} \pi a \sum_{n=0}^{\infty} \left[A_n e^{(1/2+n)\xi_2} + B_n e^{-(\frac{1}{2}+n)\xi_2} \right] e^{-(\frac{1}{2}+n)\xi_2} \\ &\quad - 8\sqrt{2} \pi a \sum_{n=0}^{\infty} \left[\left(\frac{1}{2} + n\right) A_n e^{(1/2+n)\xi_2} - \left(\frac{1}{2} + n\right) B_n e^{-(\frac{1}{2}+n)\xi_2} \right] \frac{e^{-(\frac{1}{2}+n)\xi_2}}{2n+1} \\ &= -8\pi\sqrt{2} a \sum_{n=0}^{\infty} A_n \end{aligned} \quad (4.59)$$

The average Nusselt number, \overline{N}_u can now be written as

$$\overline{N}_u = -\frac{2\sqrt{2} \sinh^2 \xi_2}{a} \sum_{n=0}^{\infty} A_n \quad (4.60)$$

which can be explicitly rewritten using equation (4.34) as

$$\overline{N}_u = -\frac{4 \sinh^2 \xi_2}{a} \sum_{n=0}^{\infty} \frac{(e^{(1+2n)\xi_1} - U_2)}{e^{(1+2n)\xi_1} - e^{(1+2n)\xi_2}} \quad (4.61)$$

4.4 VERIFICATION OF THE SOLUTION

As the distance between the two spheres increases, the effect of the existence of one sphere on the other becomes negligible. Consider, for example, two spheres having the same diameters ($r_1 = r_2$). Consider further, for simplicity, that the temperature of the top sphere is also unity ($U_2 = 1$). Then

$$\xi_1 = -\xi_2 \quad (4.62)$$

and

$$a = \frac{\sqrt{H^2 - 4r_2^2}}{2} \quad (4.63)$$

Equations (4.29), (4.30) and (4.31) reduce, respectively, to

$$A_n = \frac{\sqrt{2}}{1 + e^{(1+2n)\xi_2}} \quad (4.64)$$

$$B_n = \frac{\sqrt{2}}{1 + e^{(1+2n)\xi_2}} \quad (4.65)$$

$$U = \sqrt{2(\cosh \xi - \cos \theta)} \sum_{n=0}^{\infty} e^{-(n+1/2)\xi} \frac{(1 + e^{(2n+1)\xi})}{(1 + e^{(2n+1)\xi_2})} P_n(\cos \theta) \quad (4.66)$$

Figure 4.6 shows the isotherms for this case of two spheres of the same size and at the same temperature. The temperature gradients are obviously lower between the two spheres ($\theta = \pi$) than at the two far edges ($\theta = 0$).

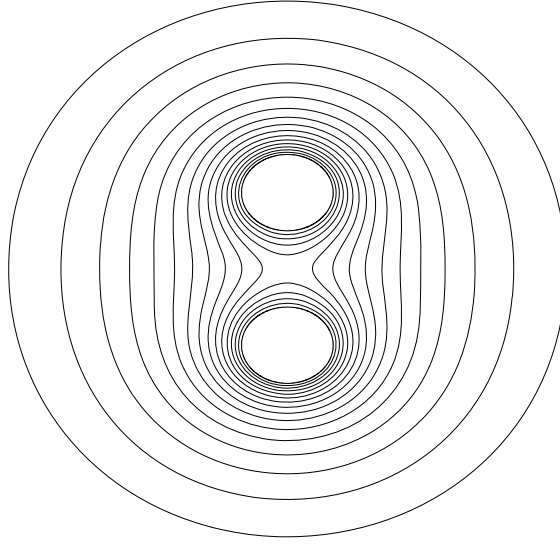


Figure 4.6. Isotherms for the case $r_1 = r_2 = 1, H = 4, U_2 = 1.0(0.05)0.3$

Isotherms shown are: 1.0, 0.95, ..., 0.3

Expression (4.36) which gives the local rate of heat transfer from the top sphere takes the following explicit form

$$N_u(\theta) = -2\sqrt{2(\cosh \xi - \cos \theta)} \times \sum_{n=0}^{\infty} \left\{ \frac{-1 - n + e^{\xi_2}(-e^{\xi_2} + e^{2n\xi_2})n + e^{(3+2n)\xi_2}(1+n) + (e^{\xi_2} - e^{2(n+1)\xi_2})(1+2n)\cos \theta}{(-1 + e^{2\xi_2})(1 + e^{(2n+1)\xi_2})} \times e^{-(n+1/2)\xi} P_n(\cos \theta) \right\} \quad (4.67)$$

With a careful investigation of the little expression (4.67), we find that as $\xi_2 \rightarrow \infty$ (i.e. the two spheres get far away from each other) the only term that contributes to the limit is that with $n = 0$, which is given as

$$\lim_{\xi_2 \rightarrow \infty} N_u(\theta) = -2 \quad (4.68)$$

Note that the sphere is hotter than the surrounding medium and the negative sign is due to the fact that the direction of increasing ξ is towards the inside of the top sphere.

Figure 4.7 shows the variation of N_u along the surface (ξ_2) for the case under consideration. As H increases, N_u becomes more uniform along the surface.

As the two spheres get far apart, the existence of one is not felt by the other. It is not surprising that one should be able to obtain the same value of N_u if the problem of a single sphere was considered in spherical coordinates. The value obtained by analyzing the problem of a single sphere in spherical coordinates is 2. [20]

The expression for the average Nusselt number (4.61), in turn, gives

$$\overline{N_u} = -\frac{4\sinh^2 \xi_2}{a} \sum_{n=0}^{\infty} \frac{(e^{-(1+2n)\xi_2} - 1)}{e^{-(1+2n)\xi_2} - e^{(1+2n)\xi_2}} \quad (4.69)$$

Figure 4.8 shows the variation of $\overline{N_u}$ along the surface (ξ_2) for the case under consideration. One can also find out that as $\xi_2 \rightarrow \infty$, the only term that contributes to the limit value is that with $n = 0$, which is given as

$$\lim_{\xi_2 \rightarrow \infty} \overline{N_u} = -2 \quad (4.70)$$

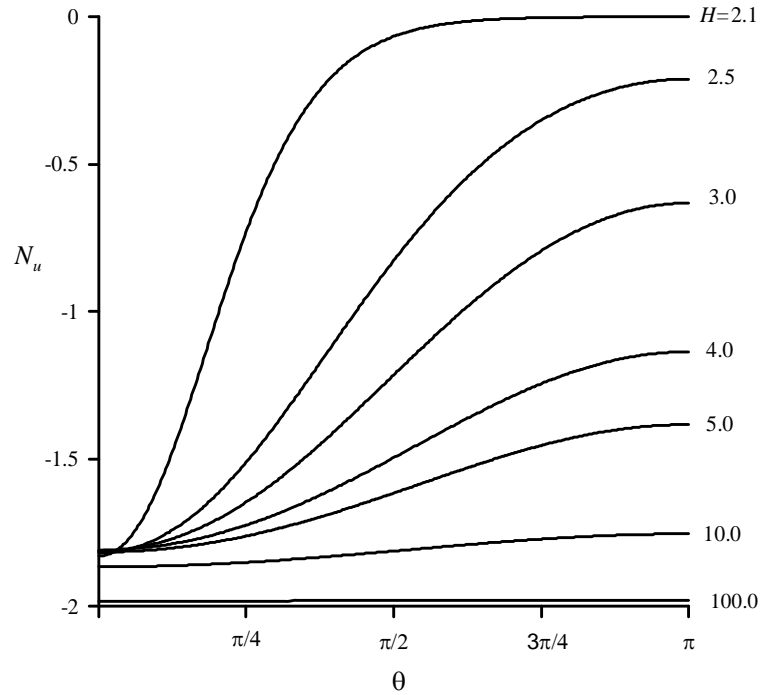


Figure 4.7. Variation of N_u along the surface (ξ_2) for the case $r_1 = r_2 = 1$ and $U_2 = 1$

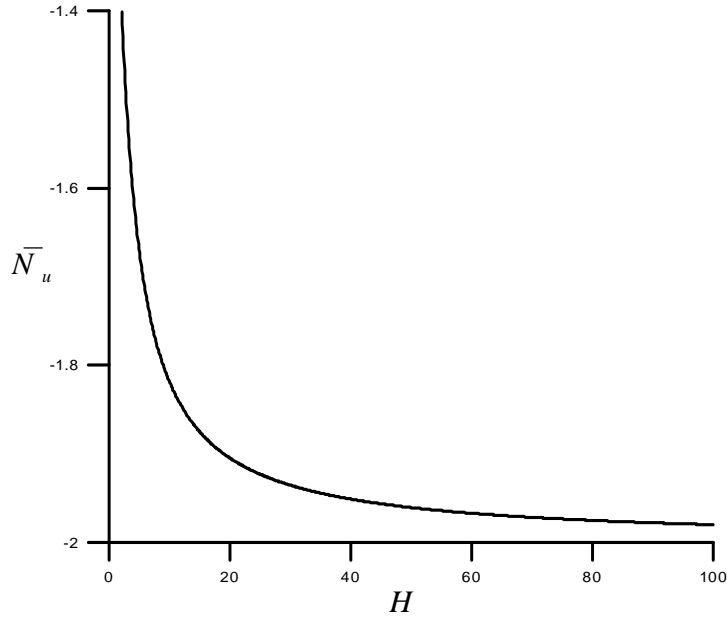


Figure 4.8. Variation of $\overline{N_u}$ along the surface (ξ_2) for the case $r_1 = r_2 = 1$ and $U_2 = 1$

4.5 TRUNCATION ERROR

We use equation (4.66) to estimate the error that results from considering only the first few terms (say N) to calculate the sum of the series solution. Due to symmetry, we consider the semi-infinite space $\xi > 0$. We can write

$$\begin{aligned} \text{Error} &= \left| \sum_{n=N+1}^{\infty} \sqrt{2(\cosh \xi - \cos \theta)} e^{-(n+1/2)\xi} \frac{(1+e^{(2n+1)\xi})}{(1+e^{(2n+1)\xi_2})} P_n(\cos \theta) \right| \\ &\leq \sum_{n=N+1}^{\infty} \sqrt{2(\cosh \xi - \cos \theta)} e^{-(n+1/2)\xi} \end{aligned} \quad (4.71)$$

as Legendre polynomials are bounded by 1, and $\frac{(1+e^{(2n+1)\xi})}{(1+e^{(2n+1)\xi_2})} \leq 1$ since $\xi \leq \xi_2$.

Since $\sqrt{2(\cosh \xi - \cos \theta)} \leq \sqrt{4 \cosh \xi} = \sqrt{2(e^\xi + e^{-\xi})} \leq \sqrt{4e^\xi} = 2e^{\xi/2}$, we can write

$$\text{Error} \leq \sum_{n=N+1}^{\infty} \sqrt{2(\cosh \xi - \cos \theta)} e^{-(n+1/2)\xi} \leq \sum_{n=N+1}^{\infty} \sqrt{2} e^{-n\xi} = 2 \frac{e^{-N\xi}}{e^{\xi} - 1} \leq 2e^{-(N+1)\xi} \quad (4.72)$$

Since the sum $\sum_{n=N+1}^{\infty} 2e^{-n\xi}$ is a geometric series and has the indicated value in (4.72).

Thus, the error decays exponentially. The results presented in this research are obtained using $N = 50$.

CHAPTER 5

EFFECT OF DIFFERENT PARAMETERS ON THE HEAT CONDUCTION PROCESS

5.1 INTRODUCTION

We consider here some cases as to understand how the heat transfer coefficient changes with the sizes of the spheres, their temperatures, and the gap between them. All values of Nusselt number refer to the top sphere.

5.2 EFFECT OF TEMPERATURE RATIO

Consider the case when we fix the radius of the two spheres and gap size (ℓ). The gap ℓ is the distance from the surface of one sphere to the surface of the other along the center-to-center line. Figure 5.1 shows the variation of N_u along the surface of the top sphere for different values of U_2 ($U_1 = 1$). In this situation the increase in U_2 decreases the local Nusselt number, N_u , around of the sphere.

Because of the direction of increasing ξ in the bispherical coordinates (towards the inside of the top sphere), positive N_u means that there is a transfer of heat to the sphere while negative values indicate that heat is transferred from the sphere to the surroundings. As expected, large thermal gradients exist in the region between the two spheres (near $\theta = \pi$) when the temperature difference is large as compared to the other regions. Negative values of U_2 ($U = (T - T_\infty) / (T_1 - T_\infty)$) indicate that the top sphere is

at temperature lower than the far field while the temperature of the lower sphere is at higher temperature than the far field or visa versa.

Figure 5.2 shows the average Nusselt number for the cases under consideration. The relation between $\overline{N_u}$ and U_2 is linear as can be seen in equation (4.61), the curves of averaged Nusselt number $\overline{N_u}$ are straight lines with negative slope.

The isotherms for some cases are shown in Figures 5.3-5.5. Notice that in Figure 5.3 when $U_2 = 0.5$, heat is transferred to the sphere through some part of the surface while heat is transferred from the sphere to the surroundings through the remaining part of the surface. In other cases, heat is completely transferred from the sphere to the surroundings ($U_2 = 3$) or transferred from the surroundings to the sphere ($U_2 = -3$).

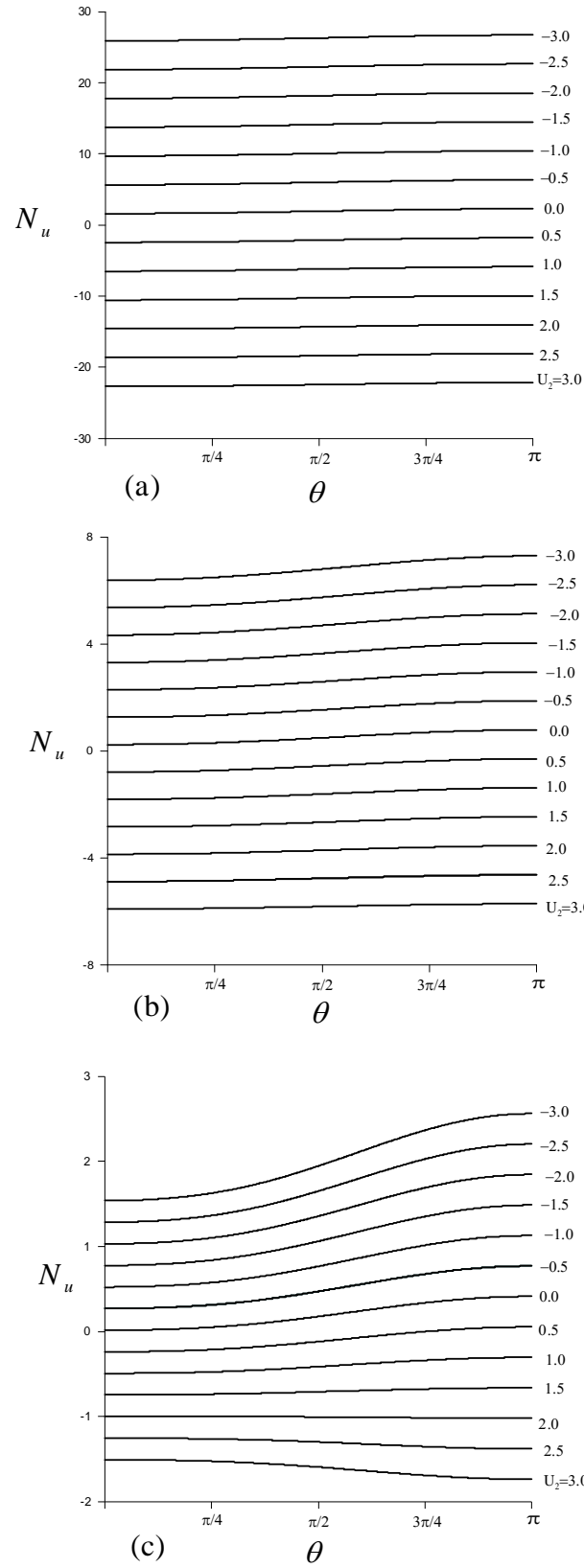


Figure 5.1. Variation of N_u along the surface (ξ_2) for the case $r_1 = 1$, $\ell = 3$, and $U_1 = 1$,

$$(a) r_2 = \frac{1}{4}, (b) r_2 = 1, (c) r_2 = 4$$

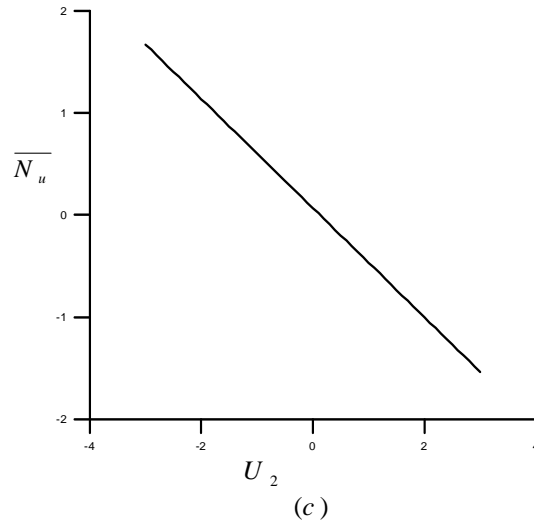
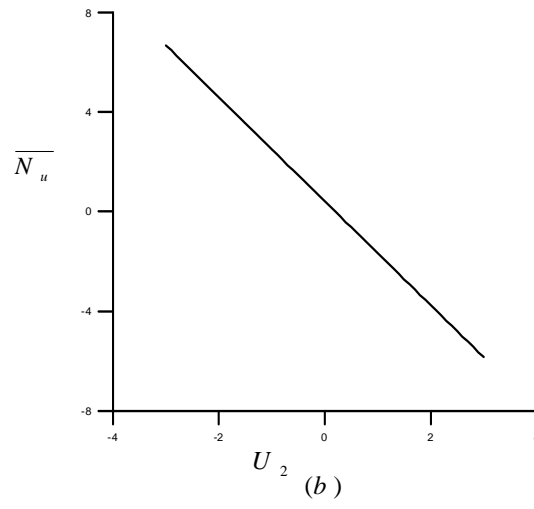
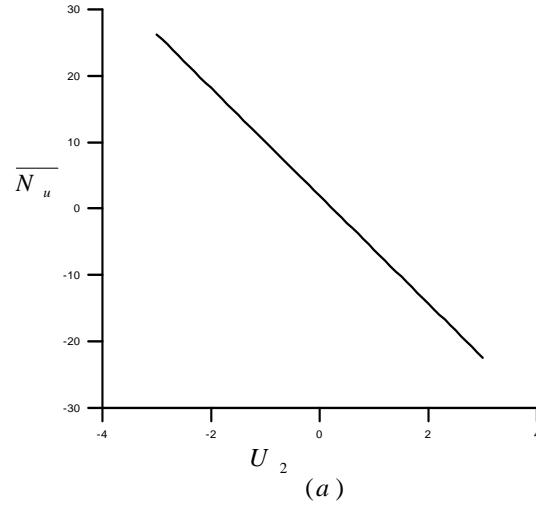


Figure 5.2. Variation of \overline{N}_u for the case $r_1 = 1, \ell = 3$,

(a) $r_2 = \frac{1}{4}$, (b) $r_2 = 1$, (c) $r_2 = 4$.

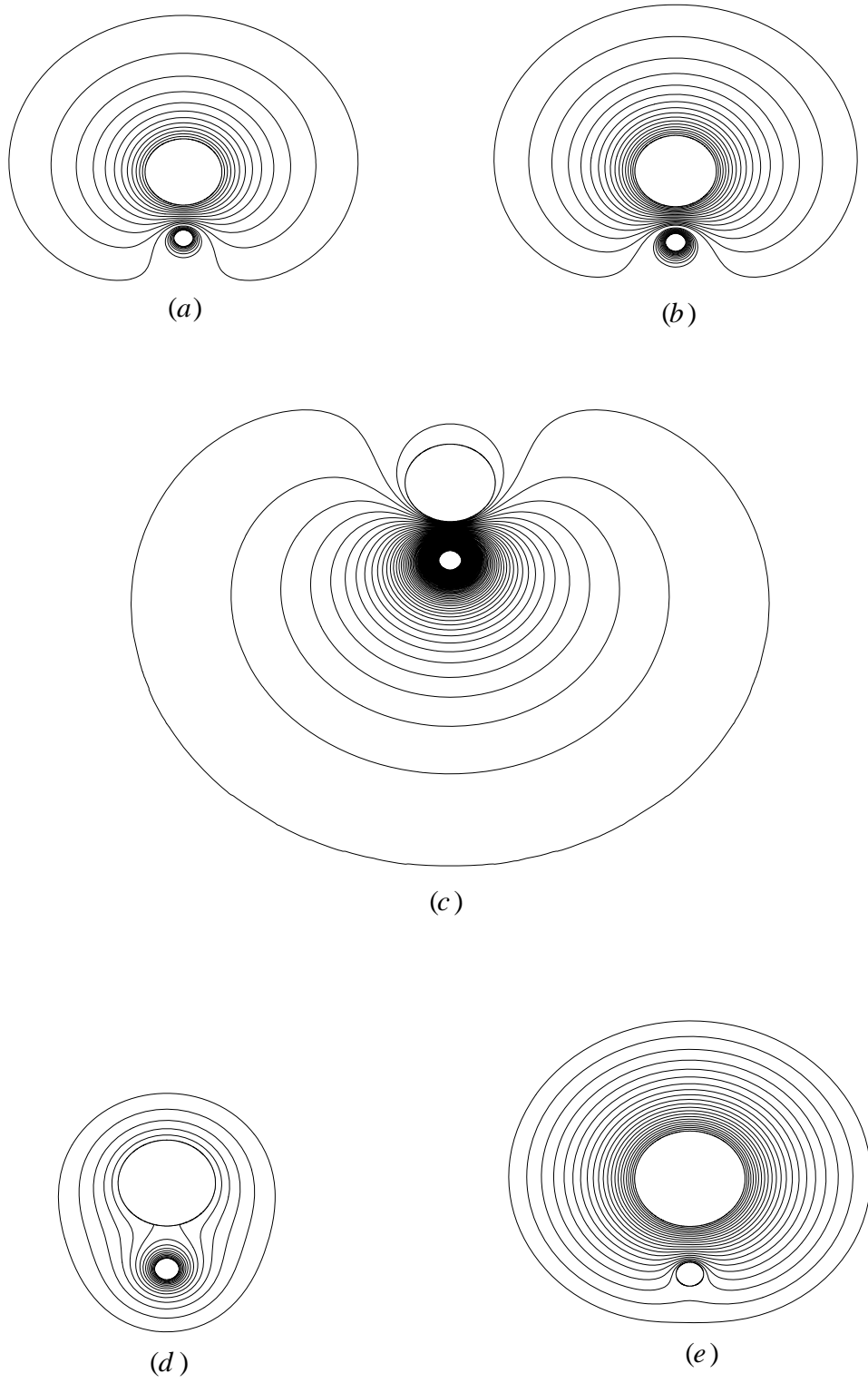


Figure 5.3. Isotherms for the case $r_1 = 1$, $r_2 = 4$, and $H = 8$

(a) $U_2 = -3.0$, (b) $U_2 = -1.0$, (c) $U_2 = 0.0$, (d) $U_2 = 0.5$, (e) $U_2 = 3.0$

Isotherms shown are: (a) $-3.0, -2.73, \dots, 0.78$ (b) $-1.0, -0.9, \dots, 0.4$

(c) $0.0, 0.009, \dots, 0.34$ (d) $0.5, 0.1, \dots, 0.25$ (e) $3.0, 2.9, \dots, 0.9$

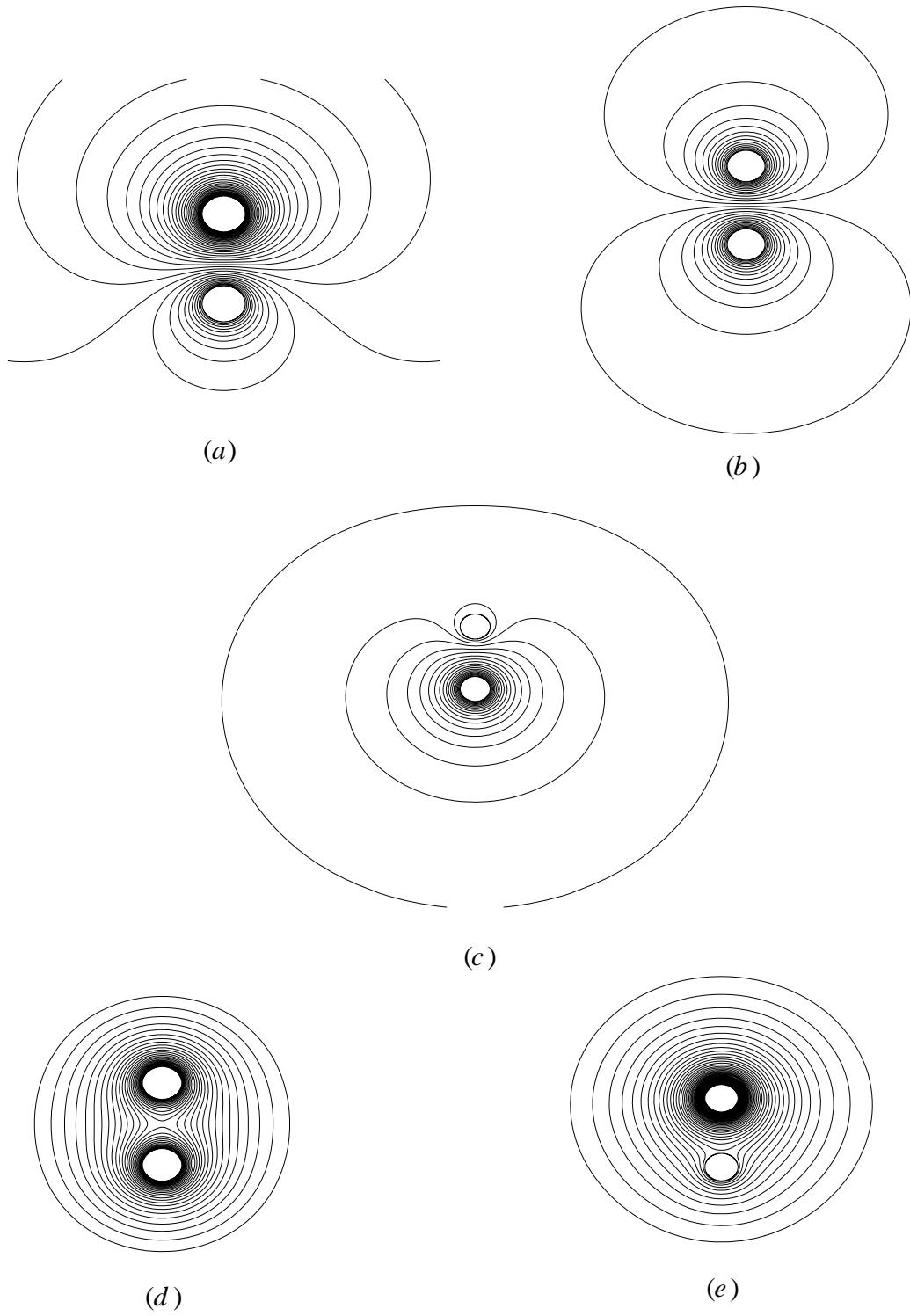


Figure 5.4. Isotherms for the case $r_1 = 1$, $r_2 = 1$, $H = 5$.

(a) $U_2 = -3.0$, (b) $U_2 = -1.0$, (c) $U_2 = 0.0$, (d) $U_2 = 1.0$, (e) $U_2 = 3.0$

Isotherms shown are: (a) $-3.0, -2.9, \dots, 1.0$ (b) $-1.0, -0.3, \dots, 0.94$

(c) $0.0, 0.05, \dots, 1.0$ (d) $1.0, 0.7, \dots, 0.24$ (e) $3.0, 2.4, \dots, 0.36$

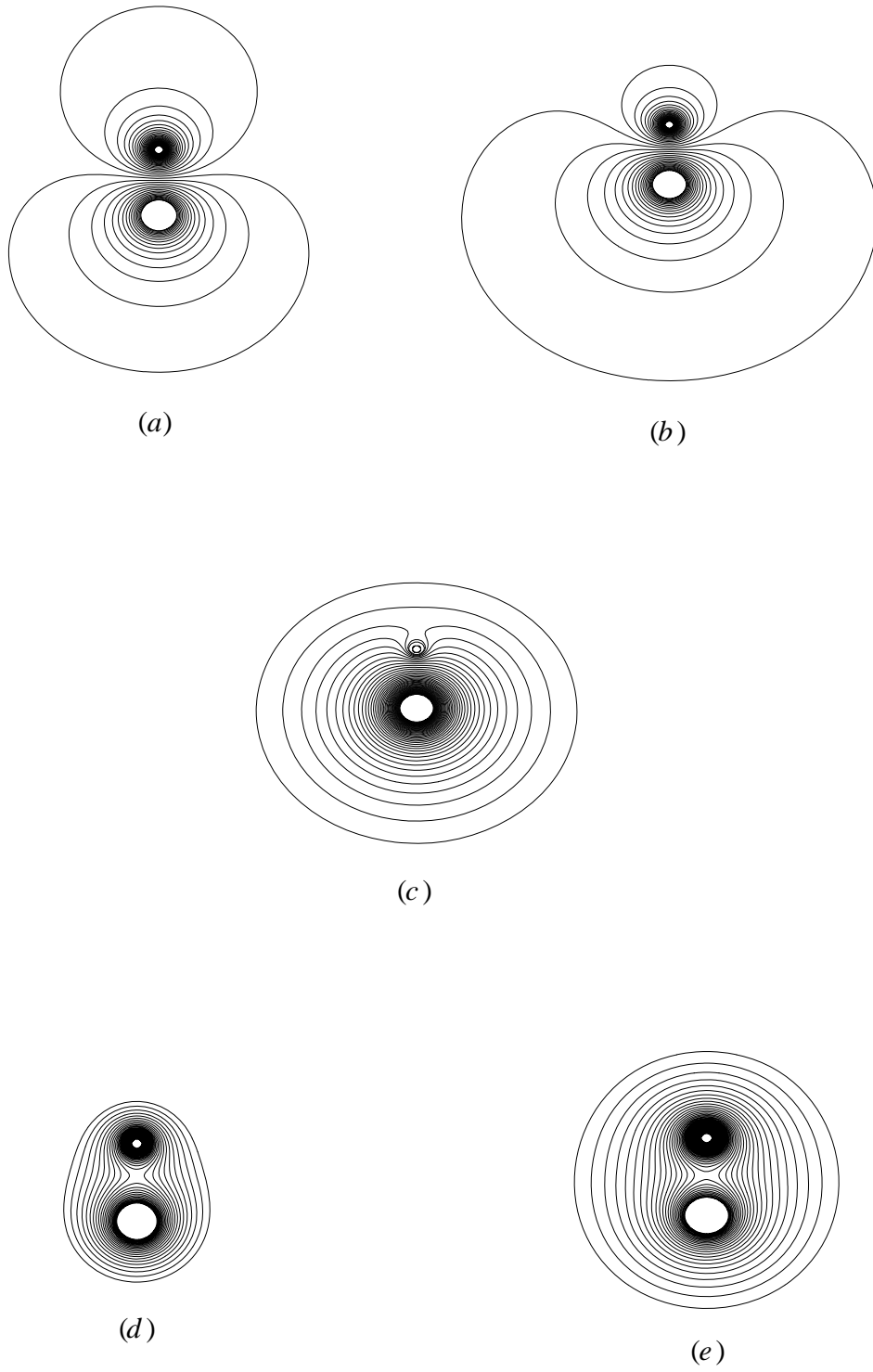


Figure 5.5. Isotherms for the case $r_1 = 1, r_2 = \frac{1}{4}, H = 4.25$.

(a) $U_2 = -3.0$, (b) $U_2 = -2.0$, (c) $U_2 = 0.0$, (d) $U_2 = 2.0$, (e) $U_2 = 3.0$

Isotherms shown are: (a) $-3.0, -2.94, \dots, 0.06$ (b) $-2.0, -1.95, \dots, 0.05$

(c) $0.0, 0.02, \dots, 0.1$ (d) $2.0, 1.73, \dots, 0.33$ (e) $3.0, 2.76, \dots, 0.03$

5.3 EFFECT OF CENTER-TO-CENTER DISTANCE

Consider the case when the temperatures of the two spheres are unchanged and the radii of the two spheres are constants. Figure 5.6 shows the variation of N_u along the surface of the top sphere for different values of H . In this case the value of N_u at the top of the top sphere ($\theta = 0$) will be almost constant over a considerable area. On the bottom of the top sphere ($\theta = \pi$), however, the increase in space between the two spheres decreases the local Nusselt number N_u values. On the other hand, as the two spheres are separated by a sufficiently large distance, each sphere behaves like an isolated one.

Figure 5.7 confirms the fact that the heat transfer coefficient approaches a constant value as the two spheres get far away from each other as expected. The figure shows the variation of the averaged Nusselt number with the center-to-center distance for the cases under consideration. As the distance increases, the existence of one sphere does not affect the other and the averaged Nusselt number approaches a constant value. The approached value is determined by the fact that we used the diameter of the bottom sphere and the temperature difference between the bottom sphere and the far field for scaling the heat transfer coefficient (Nusselt number). It is interesting to observe how $\overline{N_u}$ changes sign as the distance between the two spheres increases. When the distance is small, the temperature of the bottom sphere is higher and heat is transferred to the top sphere ($\overline{N_u} > 0$). As the distance increases, the top sphere gets free of the influence of the bottom sphere. Since the temperature of the top sphere is still higher than the far field, heat is transferred from the top sphere to the surroundings ($\overline{N_u} < 0$). Figures 5.8-5.10 shows some isotherms of this case.

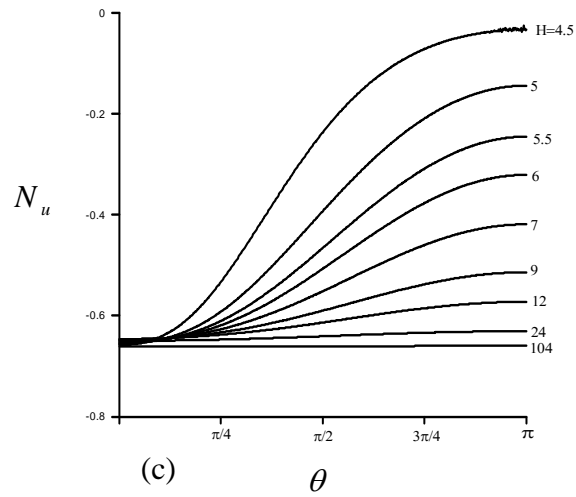
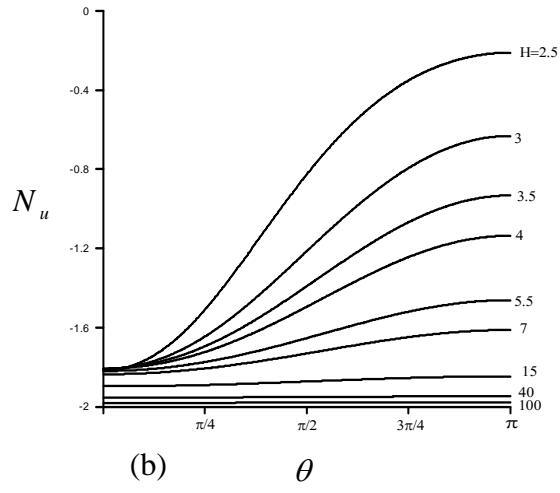
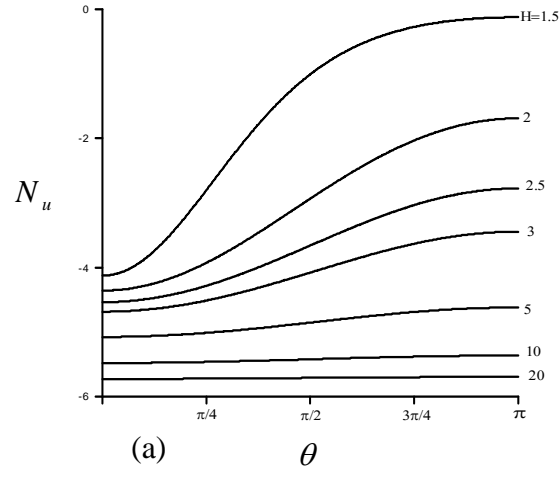


Figure 5.6. Variation of N_u along the surface (ξ_2) for the case $r_1 = 1, U_2 = 1$

(a) $r_2 = \frac{1}{3}$, (b) $r_2 = 1$, (c) $r_2 = 3$.

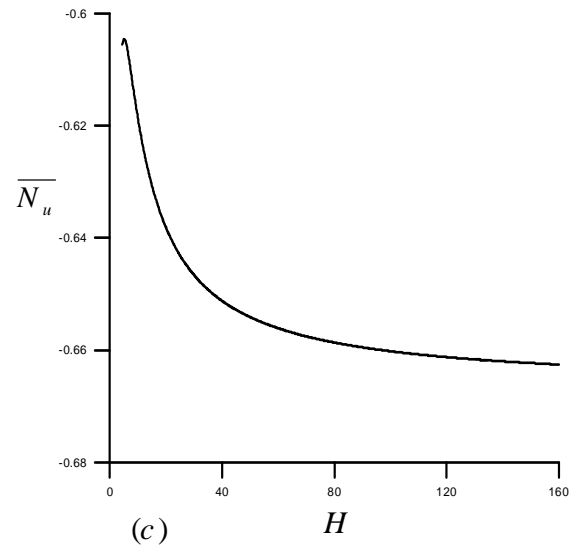
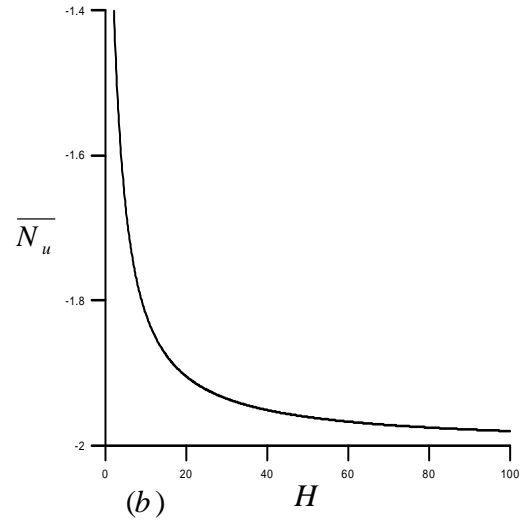
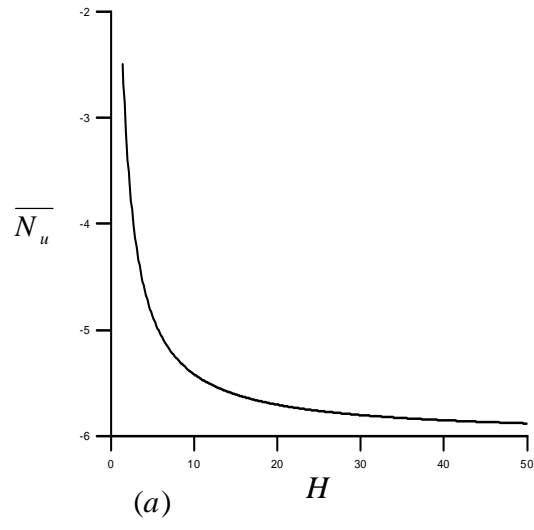
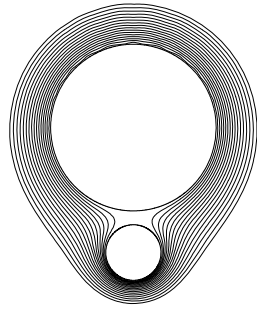


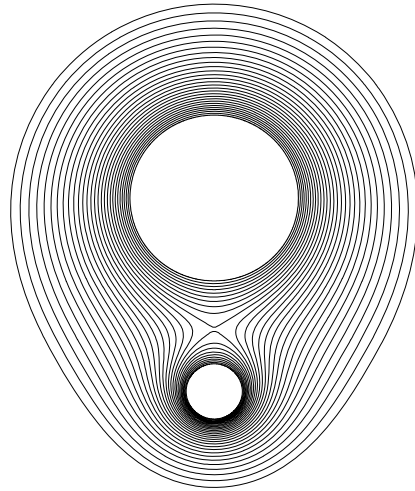
Figure 5.7. Variation of $\overline{N_u}$ for the case $r_1 = 1, U_2 = 1$

(a) $r_2 = \frac{1}{3}$, (b) $r_2 = 1$, (c) $r_2 = 3$.



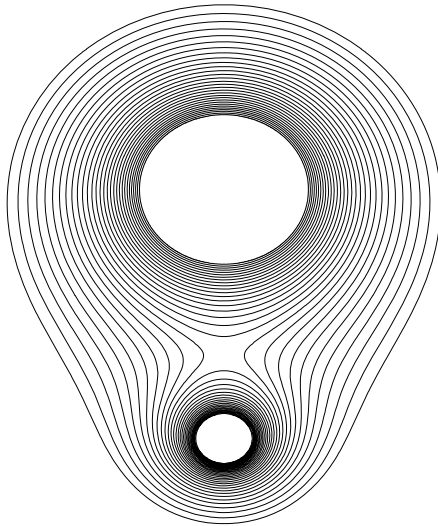
Isotherms shown are : 1.0, 0.98, ..., 0.48

(a)



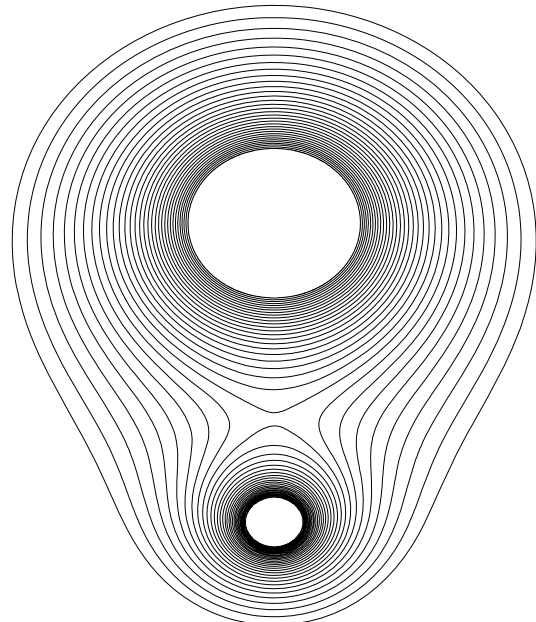
Isotherms shown are : 1.0, 0.98, ..., 0.32

(b)



Isotherms shown are : 1.0, 0.98, ..., 0.26

(c)

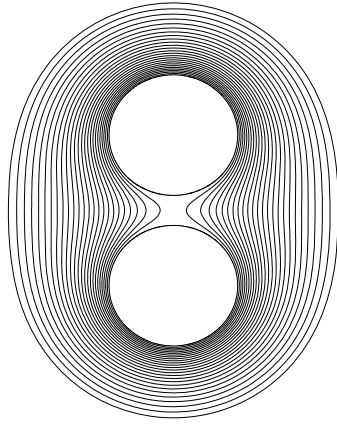


Isotherms shown are : 1.0, 0.98, ..., 0.26

(d)

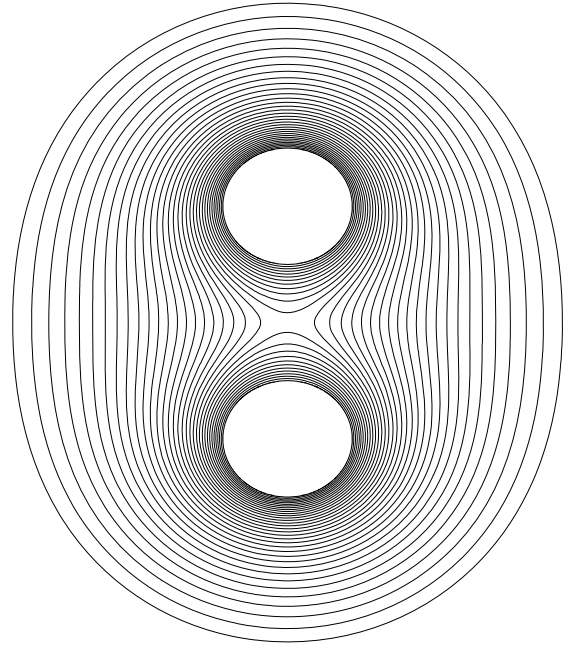
Figure 5.8. Isotherms for the case $r_1 = 1, r_2 = 3, U_2 = 1$.

(a) $H = 4.5$, (b) $H = 7$, (c) $H = 10$, (d) $H = 12$.



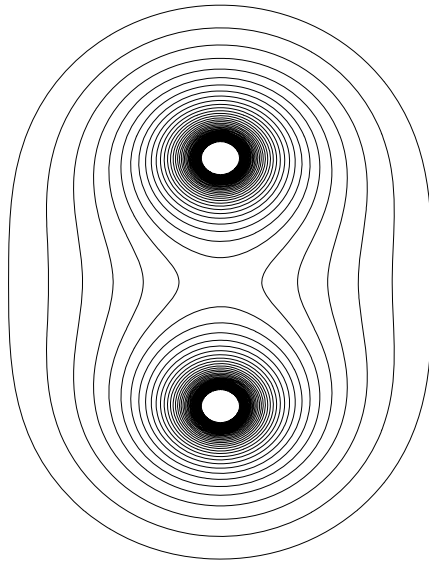
Isotherms shown are : 1.0, 0.98, ..., 0.5

(a)



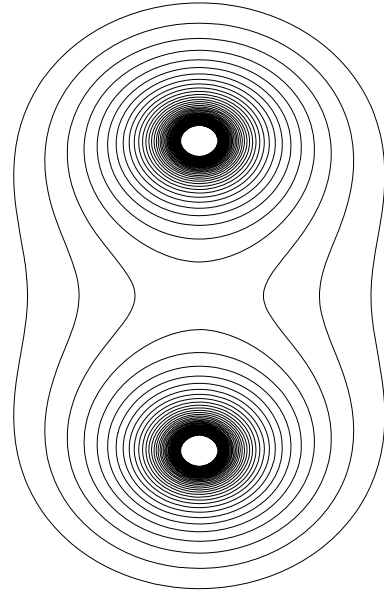
Isotherms shown are : 1.0, 0.98, ..., 0.34

(b)



Isotherms shown are : 1.0, 0.98, ..., 0.14

(c)

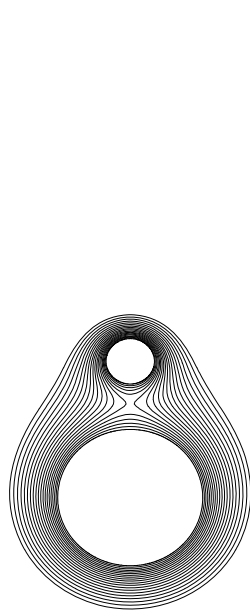


Isotherms shown are : 1.0, 0.98, ..., 0.14

(d)

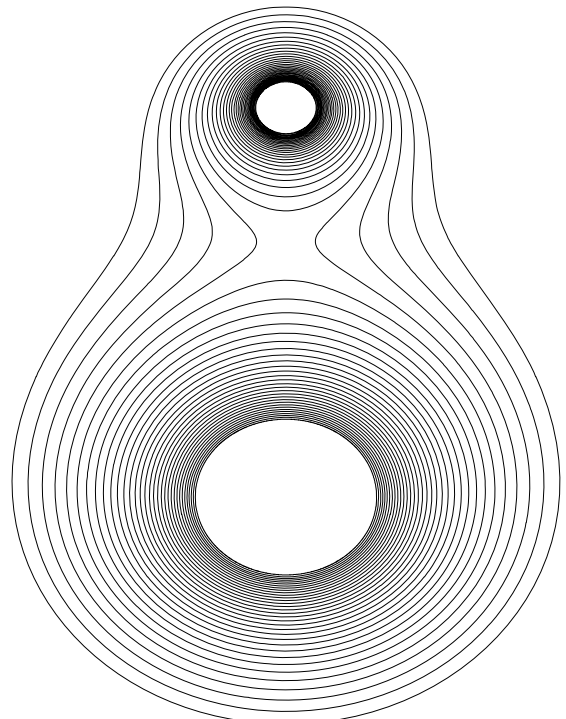
Figure 5.9. Isotherms for the case $r_1 = 1, r_2 = 1, U_2 = 1$.

(a) $H = 2.5$, (b) $H = 4$, (c) $H = 15$, (d) $H = 20$.



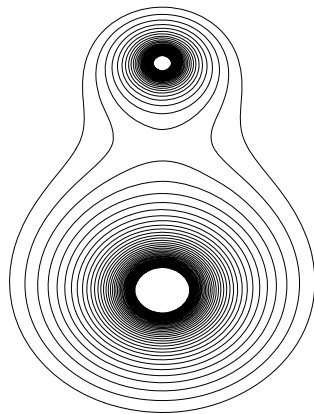
Isotherms shown are : 1.0, 0.98, ..., 0.62

(a)



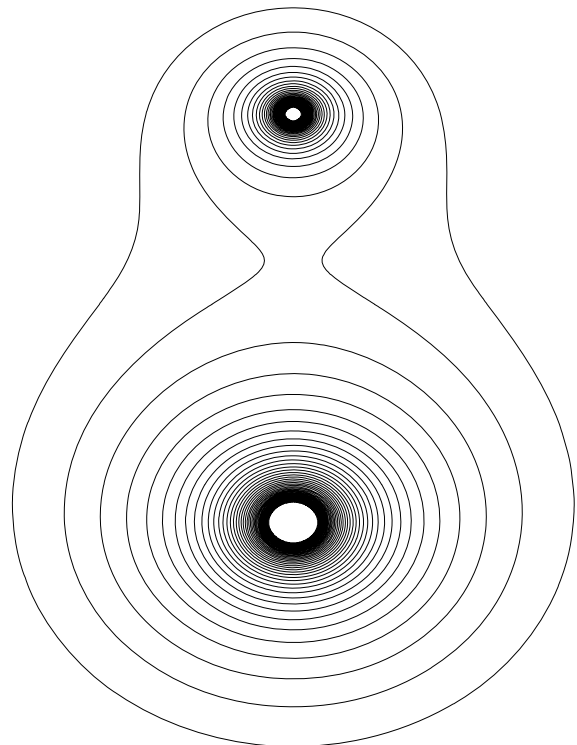
Isotherms shown are : 1.0, 0.98, ..., 0.36

(b)



Isotherms shown are: 1.0, 0.98, ..., 0.2

(c)



Isotherms shown are : 1.0, 0.98, ..., 0.1

(d)

Figure 5.10. Isotherms for the case $r_1 = 1, r_2 = \frac{1}{3}, U_2 = 1$.

(a) $H = 2$, (b) $H = 5$, (c) $H = 10$, (d) $H = 20$.

5.4 EFFECT OF RADII RATIO

Consider the case when the temperatures of the two spheres and the gap size are unchanged. Figure 5.11 shows the variation of N_u along the surface of the top sphere for different values of r_2 . In this situation, the increase in radius of the top sphere r_2 increases the local Nusselt number N_u values .

Figure 5.12 shows the averaged Nusselt number variation with the radius of the top sphere for the cases under consideration. As the diameter of the top sphere becomes large, the impact of the gap on the heat transfer rate subsides. This is expected as the gap size relative to the size of the sphere becomes small. Figure 5.13 shows some isotherms of the case $r_1 = 1, \ell = 2, U_2 = 1$.

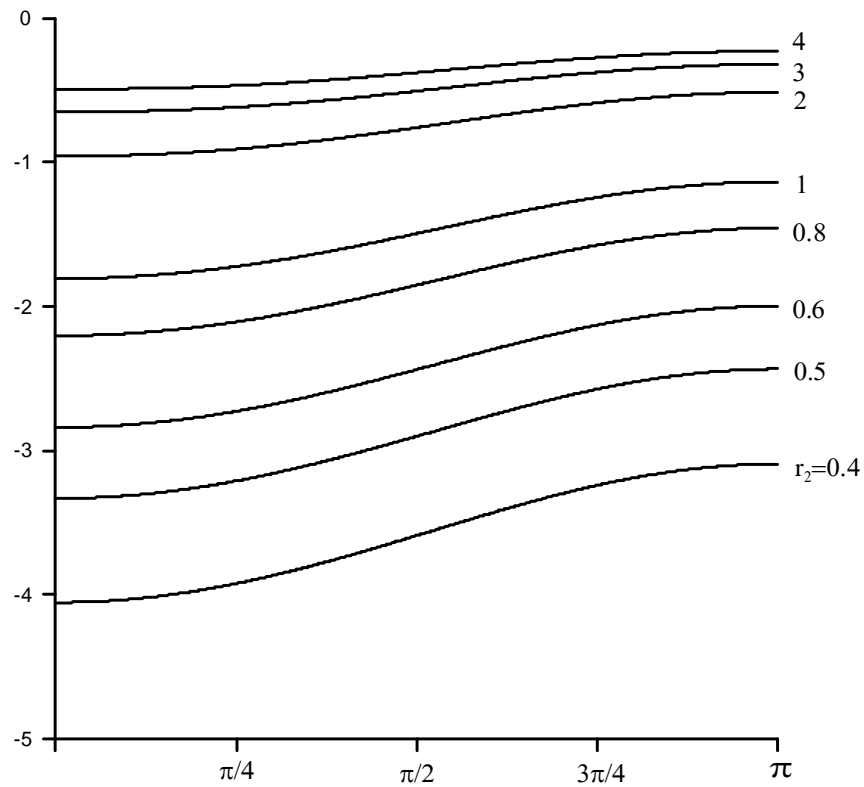


Figure 5.11. Variation of N_u along the surface (ξ_2) for the case $r_1 = 1, \ell = 2, U_2 = 1$

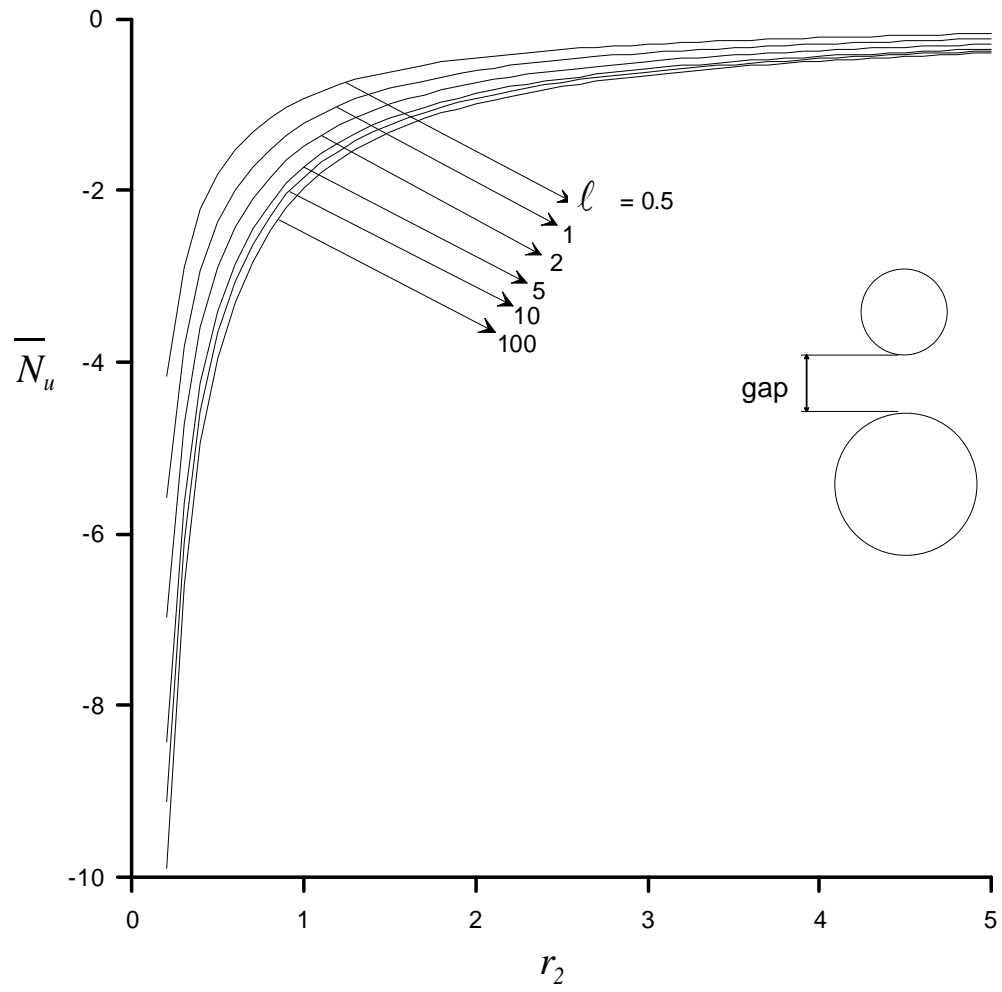
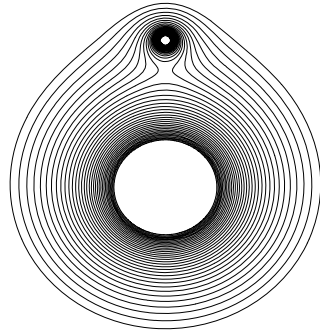
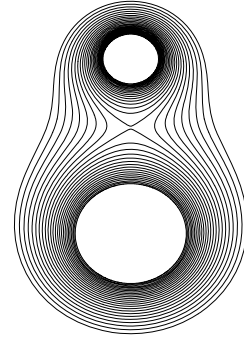


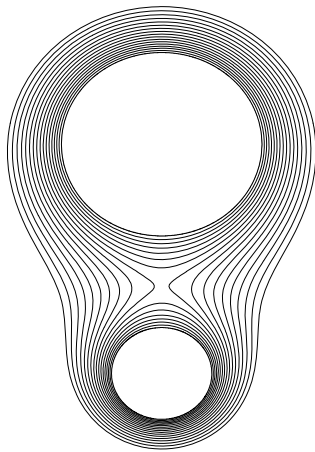
Figure 5.12. Variation of $\overline{N_u}$ with r_2 for the case $r_1 = 1$, and $U_2 = 1$



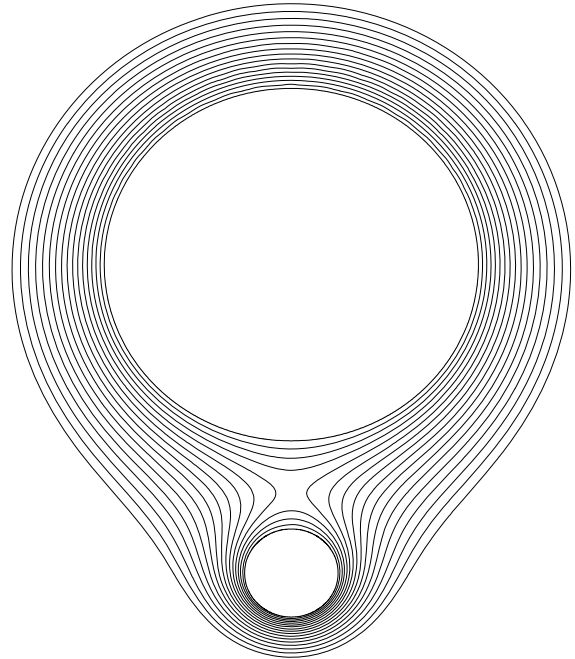
Isotherms shown are : 1.0, 0.98, ..., 0.3
(a)



Isotherms shown are : 1.0, 0.98, ..., 0.28
(b)



Isotherms shown are : 1.0, 0.98, ..., 0.58
(c)



Isotherms shown are : 1.0, 0.98, ..., 0.52
(d)

Figure 5.13. Isotherms for the case $r_1 = 1$, $\ell = 2$, $U_2 = 1$.

(a) $r_2 = 0.1$, (b) $r_2 = 0.5$, (c) $r_2 = 2$, (d) $r_2 = 4$.

CHAPTER 6

CONCLUSION AND RECOMMENDATIONS

An exact solution is obtained for the problem of heat conduction from two isothermal spheres, possibly of different diameters and different temperatures, placed at some distance from each other in a fluid of infinite extent. The unconventional bispherical coordinates system was used to solve the problem. The solution is based on a Legendre series approximation. The truncation error of this series solution was found to decay exponentially. The explicit expressions of the local and average Nusselt numbers are given respectively by equations (4.36) and (4.61). The results of the present study are verified by comparing the value of the rate of heat transfer in the case when the distance between the two spheres becomes very large to the value obtained by analyzing the problem of heat transfer from a single sphere using spherical coordinates. A parametric study was carried out for the effects of the axis ratio of the two spheres, the temperature ratio, and the center-to-center distance on the heat transfer process.

In this study, only isothermal spheres have been considered. A future research may consider constant heat flux or transient heat transfer especially when one sphere is fixed while the other is moving. This may have practical applications such as that of a moving heat source.

REFERENCES

- [1] J. M. Potter and N. Riley, Free convection from a heated sphere at large Grashof number, *J. Fluid Mech*, Vol. 100, part 4, pp. 769-783 (1980).
- [2] S. N. Brown and C. J. Simpson, Collision phenomena in free-convective flow over a sphere. *J. Fluid Mech*, Vol. 124, pp. 123-137 (1982).
- [3] F. Geoola and A. R. H. Cornish, Numerical solution of steady-state free convective heat transfer from a solid sphere, *Int. J. Heat Mass Transfer*, vol.24, No.8, pp. 1369-1379 (1981).
- [4] F. Geoola and A. R. H. Cornish, Numerical simulation of free convective heat transfer from a sphere, *Int. J. Heat Mass Transfer*, vol.25, No.11, pp. 1677-1687 (1982).
- [5] S. N. Singh. and M .M. Hasan, Free convection about a sphere at small Grashof number. *Int. J. Heat Mass Transfer*, Vol. 26, No. 5, pp. 781-783 (1983).
- [6] N. Riley, The heat transfer from a sphere in free convective flow. *Computers and Fluids*, Vol. 14, No. 3, pp. 225-237(1986).
- [7] D. R. Dudek, T. H. Fletcher, J. P. Longwell, and A. F. Sarofim, Natural convection induced forces on spheres at low Grashof numbers: comparison of theory with experiment. *Int. J. Heat Mass Transfer*, Vol. 31, No.4, pp.863- 873(1988).
- [8] S. C. R. Dennis and M. S. Walker, Forced convection from heated spheres. *Aeronautical Res. Council*, No. 26, 105(1964).
- [9] S. Whitaker, Forced convection heat transfer correlations for flow in pipes, past flat plates, single cylinders, single spheres, and for flow in packed beds and tube bundles, *AIChE J.*, Vol. 18, No. 21, 361(1972).

- [10] S. C. R. Dennis, J. D.A. Walker and J. D. Hudson, Heat transfer from a sphere at low Reynolds numbers, *J. Fluid Mech.* Vol. 60, part 2, pp. 273-283(1973).
- [11] N. N. Sayegh and W. H. Gauvin, Numerical analysis of variable property heat transfer to a single sphere in high temperature surroundings, *AIChE J.*, Vol. 25, No. 3, pp. 522-534(1979).
- [12] C. A. Hieber and B. Gebhart, Mixed convection from a sphere at small Reynolds and Grashof numbers, *J. Fluid Mech.*, Vol. 38, pp. 137-159(1969).
- [13] A. Acrivos, on the combined effect of forced and free convection heat transfer in laminar boundary layer flows, *Chem. Eng. Sci.*, Vol. 21, pp. 343-352(1966).
- [14] K-L. Wong, S.C. Lee and C-K. Chen, Finite element solution of laminar combined convection from a sphere, *ASME Journal of Heat Transfer*, Vol. 108, pp. 860-865(1986).
- [15] H.D. Nguyen, S. Paik and J.N. Chung, Unsteady mixed convection heat transfer from a solid sphere: the conjugate problem, *Int. J. Heat Mass Transfer*, Vol. 36, No. 18, pp. 4443-4453(1993).
- [16] C. K. Drummond and F. A. Lyman, Mass transfer from a sphere in an oscillating flow with zero mean velocity, *Comput. Mech.*, 6, pp.315-326(1990).
- [17] M.Y. Ha and S.Yavuzkurt, A theoretical investigation of acoustic enhancement of heat and mass transfer 1. Pure oscillating flow, *Int. J. Heat Mass Transfer*, Vol. 36, No. 8, pp. 2183-2192(1993).
- [18] R. S. Alassar, H. M. B. Badr and H. A. Mavromatis, Heat convection from a sphere placed in an oscillating free stream, *Int. J. Heat Mass Transfer*, Vol. 42, pp. 1289-1304(1999).
- [19] W.W. Leung and E.C. Baroth, An experimental study using flow visualization on the effect of an acoustic field on heat transfer from spheres, *Symposium on*

Microgravity Fluid Mechanics, FED, Vol. 42, (The American Society of Mechanical Engineers, USA).

[20] R. S. Alassar, Heat conduction from a spheroids, ASME Journal of Heat Transfer, Vol. 121, pp. 497-499(1999).

[21] Y. Solomentsev, D. Velegol and J. L. Anderson, Conduction in the small gap between two spheres, Phys. Fluids, Vol. 9, No. 5, May 1997.

[22] R. D. Stoy, Solution procedure for Laplace equation in bispherical coordinates for two spheres in a uniform external field: Perpendicular orientation, J. Appl. Phys, Vol. 66, No. 10(1989).

[23] Gheorghe Juncu, Unsteady forced convection heat/mass transfer around two spheres in tandem at low Reynolds numbers, International Journal of Thermal Sciences, Vol. 46, pp. 1011-1022(2007).

[24] R. T. Thau, D. N. Lee and W. A. Sirigano, Heat and momentum transfer around a pair of spheres in viscous flow, Int. J. Heat Mass Transfer, Vol. 27, No. 11, pp. 1953-1962(1984).

[25] V. A. Koromyslov and A. I. Grigor'ev, On the Polarization Interaction between Two Closely Spaced Conducting Spheres in a Uniform Electrostatic Field, Technical Physics, Vol. 47, No. 10, pp. 1214-1218(2002).

[26] A. Umemura, S. Ogawa and N. Oshima, Analysis of the Interaction Between Two burning Droplets, Combustion and Flame, Vol. 41, pp. 45-55(1981).

[27] A. Umemura, S. Ogawa and N. Oshima, Analysis of the Interaction Between Two burning Fuel Droplets with Different Sizes, Combustion and Flame, Vol. 43, pp. 111-119(1981).

- [28] T. A. Brzustowski, E. M. Twardus, S. Wojcicki and A. Sobiesiak, Interaction of Two burning Fuel Droplets of arbitrary Size, AIAA Journal, Vol. 17, No. 11, pp. 1234-1242(1979).
- [29] A. Cornish, Note on minimum possible rate of heat transfer from a sphere when other spheres are adjacent to it, TRANS. INSTN CHEM. ENGRS, vol. 43, pp. T332-T333 (1975).
- [30] G. Arfken, Mathematical Methods for Physicists, Academic Press, London (1970).
- [31] M. Necati Ozisik, Heat conduction, John Wiley & Sons, Inc., New York (1993).
- [32] H. F. Davis and A. D. Snider, Introduction to vector analysis, Allyn and Bacon, Inc., 470 Atlantic avenue, Boston (1979).
- [33] P. Moon, and D. E. Spencer, Field Theory Handbook, Including Coordinate Systems, Differential Equations, and Their Solutions, 2nd ed. New York: Springer-Verlag, pp. 1-48, (1988).
- [34] I. S. Gradshtyen, I. M. Ryzhik, Tables of integrals, Series and Products, 5th edition, Academic Press, (1994).
- [35] M. P. Coleman, An introduction to partial differential equations with MATLAB, CRC Press LLC, Florida (2005).
- [36] Y. Yener and S. Kakac, Heat Conduction, 4th edition, Taylor & Francis Group, LLC, New York, (2008).

VITA



Name: Basim Jamil Mohammad Al-Minshawi

Nationality: Jordanian

Date of birth: March 16, 1972

Place of birth: Jordan-Baqa

Qualification: B.A. degree in mathematics from Mua'tah University, Jordan in 2001.

M.S. degree in Mathematics from King Fahd University of Petroleum
And Minerals, Dhahran, Saudi Arabia in May, 2010.

Positions: 2001-Present: Math Teacher, Saudi Arabia
1996-2001: Math Teacher, Jordan

E-mail: balminshawi@yahoo.com

P.O. Box 5080, Dhahran 31261, Saudi Arabia